

# End Cover for Initial Value Problem: Complete Validated Algorithms with Complexity Analysis

Bingwei Zhang\*

The Courant Institute of Mathematical Sciences  
New York, USA  
bz2517@nyu.edu

Chee Yap\*†

The Courant Institute of Mathematical Sciences  
New York, USA  
yap@cs.nyu.edu

## Abstract

We consider the first order autonomous differential equation (ODE)  $\mathbf{x}' = \mathbf{f}(\mathbf{x})$  where  $\mathbf{f} : \mathbb{R}^n \rightarrow \mathbb{R}^n$  is locally Lipschitz. For a box  $B_0 \subseteq \mathbb{R}^n$  and  $h > 0$ , the set of solutions  $\mathbf{x} : [0, h] \rightarrow \mathbb{R}^n$  that satisfies  $\mathbf{x}'(t) = \mathbf{f}(\mathbf{x}(t))$  and  $\mathbf{x}(0) \in B_0$  is denoted  $\text{IVP}_f(B_0, h)$ . We provide a complete validated algorithm for the following **End Cover Problem**: given  $(\mathbf{f}, B_0, \varepsilon, h)$ , to compute a finite set  $C$  of boxes such that

$$\text{End}_f(B_0, h) \subseteq \bigcup_{B \in C} B \subseteq \left( \text{End}_f(B_0, h) \oplus [-\varepsilon, \varepsilon]^n \right)$$

where  $\text{End}_f(B_0, h) = \{\mathbf{x}(h) : \mathbf{x} \in \text{IVP}_f(B_0, h)\}$ . Moreover, we will give complexity analysis of our algorithm, and introduce a novel technique to compute End Cover  $C$  based on covering the boundary of  $\text{End}_f(B_0, h)$ . Finally, we give experimental results indicating the practicality of our techniques.

## Keywords

initial value problem, IVP, end cover problem, reachability problem, end-enclosure problem, validated algorithms, interval methods, logarithmic norm, matrix measure,

## ACM Reference Format:

Bingwei Zhang and Chee Yap. 2026. End Cover for Initial Value Problem: Complete Validated Algorithms with Complexity Analysis. In . ACM, New York, NY, USA, 15 pages. <https://doi.org/XXXXXX.XXXXXXX>

## 1 Introduction

The initial value problem (IVP) for ordinary differential equations leads to challenging computational problems. A chief reason is that approximation errors typically grow exponentially large with time. So simulating an IVP over a long time span will break down. Other difficulties include the presence of singularities as well as the phenomenon of stiffness (regions where the solution changes quickly). Although numerical algorithms based on machine precision have been very successful in practice, there remains a need for certifiable or **validated algorithms**. Such algorithms have been considered

\*Both authors contributed equally to this research.

†Corresponding author

Permission to make digital or hard copies of all or part of this work for personal or classroom use is granted without fee provided that copies are not made or distributed for profit or commercial advantage and that copies bear this notice and the full citation on the first page. Copyrights for components of this work owned by others than the author(s) must be honored. Abstracting with credit is permitted. To copy otherwise, or republish, to post on servers or to redistribute to lists, requires prior specific permission and/or a fee. Request permissions from [permissions@acm.org](mailto:permissions@acm.org).

Conference'17, Washington, DC, USA

© 2026 Copyright held by the owner/author(s). Publication rights licensed to ACM. ACM ISBN 978-1-4503-XXXX-X/2018/06  
<https://doi.org/XXXXXX.XXXXXXX>

from the beginning of interval analysis over 50 years ago [1]. Unfortunately, many validated algorithms in this area are only **partially correct** in the sense that, if they halt, then the output is validated [2]. But halting of validated algorithms are rarely addressed. Thus the challenge is to construct **complete validated algorithms**, i.e., halting ones.

In this paper, we consider the following system of first order ordinary differential equations (ODEs)

$$\mathbf{x}' = \mathbf{f}(\mathbf{x}) \quad (1)$$

where  $\mathbf{f} = (f_1, \dots, f_n) : \mathbb{R}^n \rightarrow \mathbb{R}^n$  is locally Lipschitz. For  $B_0 \subseteq \mathbb{R}^n$  and  $h > 0$ , let  $\text{IVP}_f(B_0, h)$  denote the set of total differentiable functions  $\mathbf{x} = (x_1, \dots, x_n) : [0, h] \rightarrow \mathbb{R}^n$  such that  $\mathbf{x}(0) \in B_0$  and the time derivative  $\mathbf{x}' = (x'_1, \dots, x'_n)$  satisfies (1). Call each  $\mathbf{x} \in \text{IVP}_f(B_0, h)$  a **solution** to the **IVP instance**  $(\mathbf{f}, B_0, h)$ . The **end slice** of  $\text{IVP}_f(B_0, h)$  is

$$\text{End}_f(B_0, h) := \{\mathbf{x}(h) : \mathbf{x} \in \text{IVP}_f(B_0, h)\}. \quad (2)$$

If  $B_1$  contains the end slice, we call  $B_1$  an **end enclosure** of  $\text{IVP}_f(B_0, h)$ . In our previous paper [2], we gave a complete validated algorithm for the **End Enclosure Problem**<sup>1</sup> which is defined by this header:

END ENCLOSURE PROBLEM:

$$\text{EndEnc}_f(B_0, \varepsilon; \mathbf{p}_0, \mathbf{h}) \rightarrow (\underline{B}_0, \bar{B}_1)$$

INPUT:  $B_0 \in \mathbb{I}\mathbb{R}^n$ ,  $\varepsilon > 0$ ,  $\mathbf{p}_0 \in B_0$ ,  $h > 0$ .

The optional arguments  $\mathbf{h}$  and  $\mathbf{p}_0$  have default values  $\mathbf{h} = 1$ ,  $\mathbf{p}_0 = m(B_0)$ .

OUTPUT:  $\underline{B}_0, \bar{B}_1 \in \mathbb{I}\mathbb{R}^n$  such that

$$\mathbf{p}_0 \in \underline{B}_0 \subseteq B_0, \text{End}_f(\underline{B}_0, h) \subseteq \bar{B}_1 \in \mathbb{I}\mathbb{R}^n, \text{ and } \max \text{ width } w_{\max}(\bar{B}_1) < \varepsilon. \quad (3)$$

Here,  $\mathbb{I}\mathbb{R}^n$  denotes the set of compact boxes in  $\mathbb{R}^n$ , and our algorithms assume that the  $B$ 's in input and output are boxes. The usual IVP formulation in the literature assumes the singleton  $B_0 = \{\mathbf{p}_0\}$ . Our formulation with box  $B_0$  (following Corliss [3, Section 3]) is more realistic since in any real application (as in biology or physics), one never know an exact point  $\mathbf{p}_0$ , only some range of interest.

A key insight for showing the halting of our algorithm is to formulate the problem (3) as a *promise problem*: the input  $(B_0, h)$  is promised to be **valid**. This means, for all  $\mathbf{p}_0 \in B_0$ , the ODE (1) has<sup>2</sup> a unique solution  $\mathbf{x} : [0, h] \rightarrow \mathbb{R}^n$  with  $\mathbf{x}(0) = \mathbf{p}_0$ . The output

<sup>1</sup>Computational problems are specified using a header of the form

$$\text{PROBLEM}(\mathbf{a}; \mathbf{b}) \rightarrow \mathbf{c}$$

where  $\mathbf{a}, \mathbf{b}, \mathbf{c}$  are sequences representing (respectively) the required arguments, the optional arguments, and the outputs. Default values for optional arguments may be directly specified (as in  $h = 1$  above) or they may be context dependent. In [2],  $\mathbf{p}_0$  was implicitly defaulted to the midpoint of  $B_0$ .

<sup>2</sup>Without such a promise, we might require the algorithm to output “invalid” when there is no solution. Such an algorithm would *a fortiori* decide whether the input is valid. This decision problem, to our knowledge, is an open problem [2].

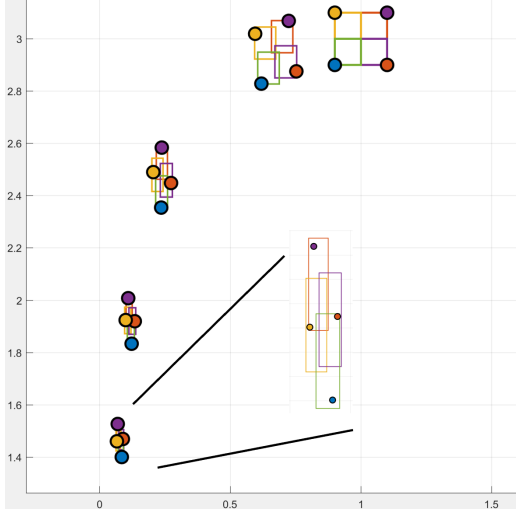


**Figure 1:**  $\varepsilon$ -End Covers ( $\varepsilon = 0.1$ ) at times  $h_i \in (0, 0.1, 0.4, 0.7, 1.0)$  for  $i = 0, \dots, 4$ . The boxes in  $C$  are colored for visualization. An enlarged image for the cover at  $h_4 = 1.0$  is also shown.

requirement that  $w(\bar{B}_1) < \varepsilon$  implies that  $B_0$  must be allowed to shrink to some  $\underline{B}_0$  (while keeping  $p_0$  in  $\underline{B}_0$ ). In this paper, we address a stronger variant of the above problem, in which the shrinkage of  $B_0$  is not allowed. This is the **End Cover Problem** which is defined by the following header:

END COVER PROBLEM:  
 $\text{EndCover}_f(B_0, \varepsilon) \rightarrow C$

---

INPUT:  $B_0 \in \mathbb{R}^n$ ,  $\varepsilon > 0$   
OUTPUT:  $C$ , an  $\varepsilon$ -end cover of  $\text{End}_f(B_0, h)$ .  
I.e.,  $C$  is a finite set of boxes such that  
 $\text{End}_f(B_0, h) \subseteq \bigcup C \subseteq \left( \text{End}_f(B_0, h) \oplus [\pm \varepsilon]^n \right)$

(4)

Here,  $[\pm \varepsilon]^n$  denotes the box  $\prod_{i=1}^n [-\varepsilon, \varepsilon]$ ,  $A \oplus B$  denotes the Minkowski sum of sets  $A, B \subseteq \mathbb{R}^n$ , and  $\bigcup C := \bigcup_{B \in C} B$  is a subset of  $\mathbb{R}^n$ . For any  $\varepsilon > 0$ , clearly  $\varepsilon$ -end covers of  $\text{End}_f(B_0, h)$  exists. Our introduction of *a priori*  $\varepsilon$ -bounds in the problems (3) and (4) is clearly highly desirable. As far as we know, current IVP algorithms do not offer such guarantees.

## 1.1 What is new in this paper

We have three main objectives: The first is to enhance our end enclosure algorithm in [2], leading to a solution for End Cover Problem (4). The issue is this: suppose we want to compute an  $\varepsilon$ -cover for the IVP instance  $(B_0, \varepsilon, h)$  where  $B_0 = [a, b]$  ( $n = 1$ ). Using our End Enclosure Algorithm, we can compute  $B_1$  that is an  $\varepsilon$ -cover of  $\text{End}_f([a, a_1], h)$  for some  $a < a_1 \leq b$ . If  $a_1 < b$ , then we repeat this process to compute a  $B_2$  to cover  $\text{End}_f([a_1, a_2], h)$  for some  $a_1 < a_2 \leq b$ , etc. If this process terminates, we have a finite  $\varepsilon$ -cover  $C = \{B_1, B_2, \dots\}$ . Viewing  $x$  as space variables, this shows that our problem is the “space cover” of  $[a, b]$ , analogous to the “time cover” of  $[0, h]$  in the original End Enclosure Problem.

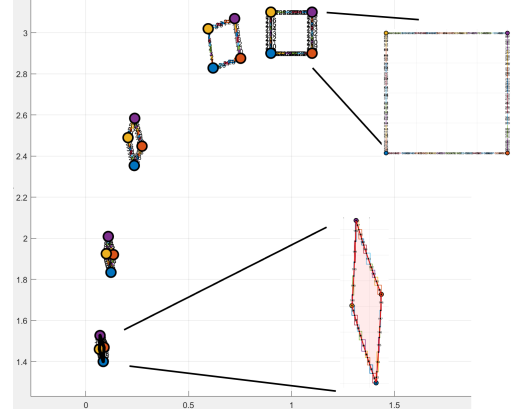


**Figure 2:**  $\varepsilon$ -Boundary Covers ( $\varepsilon = 0.01$ ) at times  $h_i \in (0, 0.1, 0.4, 0.7, 1.0)$  for  $i = 0, \dots, 4$ . The boxes in a cover  $C$  are colored to visualize them. An enlarged image for the cover at  $h_4 = 1.0$  is also shown.

In Figure 1, we show the output of our end cover algorithm on the Volterra-Lottke (or predator-prey) system (Table 1, Section 5) with  $\varepsilon = 0.1$ . We show five IVP instances ( $i = 0, \dots, 4$ )

$$(f, B_0, h_i, \varepsilon) = \left( \begin{bmatrix} 2x(1-y) \\ -y(1-x) \end{bmatrix}, \text{Box}_{(1,3)}(0.1), h_i, 0.1 \right)$$

where  $h_i \in (0, 0.1, 0.4, 0.7, 1.0)$  and  $\text{Box}_p(w)$  denotes box  $p + [-w, w]^2$ .

Our second objective is to introduce a boundary cover technique to solve the End Cover Algorithms. The basic idea is to reduce the covering of  $\text{End}_f(B_0, h)$  to the covering of its boundary,  $\partial(\text{End}_f(B_0, h))$ . Any  $\varepsilon$ -cover of  $\partial(\text{End}_f(B_0, h))$  is called an  **$\varepsilon$ -boundary cover** of  $\text{End}_f(B_0, h)$ . Thus we reduce the  $n$ -dimensional problem to a  $(n-1)$ -dimensional one, modulo a **filling problem**: given  $C$ , an  $\varepsilon$ -boundary cover of  $\text{End}_f(B_0, h)$ , to compute a finite set of boxes  $C_0$  so that  $C \cup C_0$  is an  $\varepsilon$ -cover of  $\text{End}_f(B_0, h)$ . In other words,  $C_0$  covers the “interior” of  $\bigcup C$ .

In Figure 2, we run our boundary cover algorithm on the same Volterra-Lottke instances of Figure 1, but with  $\varepsilon = 0.01$  instead of  $\varepsilon = 0.1$ . The running time is much faster than that. The filling problem to convert  $C_i$  into an end cover of  $\text{End}_f(B_0, h_i)$  is relative easy for these instances because the “interior polygon” (pink area in the enlarged image) of  $C_i$  are simple polygons. We reduced  $\varepsilon$  to 0.01 (from the previous 0.1) to ensure the interior polygons are non-empty. Despite the smaller  $\varepsilon$ , the boundary computation is much faster than the end cover computation.

Although the boundary method seems like a natural suggestion, its justification depends on a non-trivial result<sup>3</sup> called the **Invariance of Domain Theorem** from L.E.J. Brouwer. We use this result to prove Section 3 that if  $B_0$  is a homeomorphic ball (e.g., a box), then  $\text{End}_f(B_0, h)$  is also a homeomorphic ball. So, if  $C$  is an  $\varepsilon$ -boundary enclosure of  $\text{End}_f(B_0, h)$ , then  $\bigcup C$  is a connected set which can be “filled” by a set  $C_0$  of boxes to give an  $\varepsilon$ -end cover, as noted above.

<sup>3</sup>See [Terry Tao's blog](#) on Brouwer's Fixed Point Theorem.

Our third objective is to give a complexity analysis of the above algorithms. Note that complexity analysis is rarely possible in validated algorithms literature for various reasons. Using the enhanced End Enclosure algorithm (Section 2.2) we can now give explicit bounds, based on implicit parameters such as logNorm bound  $\bar{\mu}$  on the input box.

## 1.2 Background and Brief Literature Review.

The computational problems associated with  $\text{End}(B_0)$  has many applications, and are often called **reachability problems** in areas as non-linear control systems and verification literature (e.g., [4, 5]). The concept of partially correct algorithms and promise problems are standard in theoretical computer science. “Partial correctness” is an extremely useful concept because it splits the correctness of algorithms into two distinct parts: halting and correct output. Promise problems [6] are natural and common in numerical computation: a typical promise is that the input is non-singular or well-conditioned. Algorithms for promise problems can assume the promised condition without checking for it.

Ultimately, validated algorithms will need arbitrary precision numerics (bigNumbers packages such as gmp). Although this is in our goal, we avoid a direct discussion of this aspect in order to focus on the main algorithmic development. Our algorithmic development in this paper follows the standard approach in numerical algorithms in which we describe an **abstract algorithm A** operating on exact mathematical operations or objects. But these abstract description must ultimately be replaced by implementable operations and representable objects. Following [7], we do this in two steps: first, we transform A to the **interval version**  $\square A$ , which computes with bounding intervals instead of exact values. But  $\square A$  may still be abstract as the interval bounds often involve real numbers. The next step converts  $\square A$  to the **effective version**  $\tilde{\square} A$  that involves only implementable operations (like bigFloats) and finite representations. The steps  $A \rightarrow \square A \rightarrow \tilde{\square} A$  are often relatively simple as the global properties are largely preserved. This A/I/E approach is outlined in [7]. But not every abstract A has a simple transformation into  $\square A$ : the main issue is when A relies on some “zero problem”. E.g., in the Gaussian elimination algorithm A for a matrix determinant, there is no simple  $\square A$  as A relies on knowledge that a pivot is non-zero. Our IVP algorithms have no such “zero problems”.

Validated algorithms for IVP’s have discussed by Moore from the beginning of interval computation; see surveys in Corliss [3] and Nedialkov et al. [8]. These algorithms follow a standard motif of repeated applications of two subroutines that Corliss called “Algorithm I” and “Algorithm II”. We call them StepA and StepB, to emphasize that they are steps in iterative algorithm. Briefly, StepA takes a (small enough) time step so that the ODE remains valid and whose full-enclosure can be estimated; StepB refines this estimate to get a tighter end-enclosure. In [2], we introduce the scaffold data structure to allow more innovative algorithmic processes to take place.

Our algorithm exploits the notion of logarithmic norms of differential equations.

Our notion of trajectory bundles in Subsection 3.1 appears to be new; but the term has appeared in contexts such as in path planning,

optimization and optics. They refer to the algorithmic technique of “multiple shooting or trajectory sampling” to better estimate the end set. E.g., [9, 10].

## 1.3 Paper Overview.

The remaining sections of this paper are as follows: In Section 2, we first establish some notations and review our previous End Enclosure algorithm. Then we describe a modification to enhance its performance. This enhanced algorithm is then used to solve the End Cover Problem. In Section 3, we introduce the Boundary Cover Problem. We prove a key result based on Brouwer’s Invariance Theorem algorithm that reduces it to End Covers in one dimension lower. We discuss how this can lead to alternative End Cover algorithm that is more accurate. In Section 4, we analyze the complexity of the algorithms in Sections 2 and 3. In Section 5, we describe some experiments on implementations of these algorithms, showing their practicality. We conclude in Section 6 and include an Appendix for proofs.

## 2 The End Cover Problem

This section will describe an enhancement of EndEncl Algorithm in [2], leading to a complete validated algorithm for the End Cover Problem. This enhancement is also needed for its complexity analysis. First, we establish some notations.

### 2.1 Notations and Basic Concepts

We collect the basic terminology here for easy reference, largely following [2]. We use bold font like  $\mathbf{p} = (p_1, \dots, p_n)$  for vectors, with  $(\mathbf{p})_i = p_i$  as the  $i$ th coordinate function. The origin in  $\mathbb{R}^n$  is denoted  $\mathbf{0} = (0, \dots, 0)$ . Let  $\square \mathbb{R}$  denote the set of compact intervals. We identify the interval  $[a, a]$  with  $a \in \mathbb{R}$  and thus  $\mathbb{R} \subseteq \square \mathbb{R}$ . For  $n \geq 1$ , let  $\square \mathbb{R}^n := (\square \mathbb{R})^n$  denote the set of (axes-aligned) boxes in  $\mathbb{R}^n$ . For a non-empty set  $S \subseteq \mathbb{R}^n$ , let  $\text{Ball}(S)$  and  $\text{Box}(S)$  denote, respectively, the smallest ball and smallest box containing  $S$ . Also, let  $\mathbf{m}(S)$  denote the midpoint of  $\text{Box}(S)$ . For  $\alpha \geq 0$ , the  $\alpha$ -dilation operator is  $\alpha S := \{\alpha \mathbf{p} : \mathbf{p} \in S\}$ . E.g., if  $n = 1$  and  $S = [2, 6]$  then  $\frac{1}{2}S = [1, 3]$ .

The  $\text{Box}$  and  $\text{Ball}$  operators in  $\mathbb{R}^n$  can also take numerical parameters:  $\text{Ball}(r)$  is the ball in  $\mathbb{R}^n$  centered at  $\mathbf{0}$  of radius  $r \geq 0$ , and  $\text{Box}(\mathbf{r}) := \prod_{i=1}^n [-r_i, r_i]$  where  $\mathbf{r} = (r_1, \dots, r_n) \geq \mathbf{0}$ . If  $\mathbf{p} \in \mathbb{R}^n$ , let  $\text{Ball}_{\mathbf{p}}(\mathbf{r}) := \mathbf{p} + \text{Ball}(\mathbf{r})$  and  $\text{Box}_{\mathbf{p}}(\mathbf{r}) := \mathbf{p} + \text{Box}(\mathbf{r})$ . Simply write  $\text{Box}(\mathbf{r})$  and  $\text{Box}_{\mathbf{p}}(\mathbf{r})$  if  $r_i = r$  for all  $i = 1, \dots, n$ . The **width** of the box  $B = \text{Box}_{\mathbf{p}}(\mathbf{r})$  is  $\mathbf{w}(B) := 2\mathbf{r}$ . The dimension of  $B \in \square \mathbb{R}^n$  is the number  $\dim(B) \in \{0, \dots, n\}$  of positive values in  $\mathbf{w}(B)$ . The **maximum, minimum widths** of  $B$  are  $w_{\max}(B) := \max_{i=1}^n (\mathbf{w}(B))_i$ , and similarly for  $w_{\min}(B)$ . The natural extension of any function  $f : X \rightarrow Y$  is used throughout; this extension (still denoted  $f$ ) is  $f : 2^X \rightarrow 2^Y$  where  $f(X) = \{f(x) : x \in X\}$  and  $2^X$  is the power set of  $X$ . If  $f : \mathbb{R}^n \rightarrow \mathbb{R}^m$ , then a **box function** for  $f$  is any function of the form  $\square f : \square \mathbb{R}^n \rightarrow \square \mathbb{R}^m$  that is conservative, i.e.,  $f(B) \subseteq \square f(B)$ , and convergent, i.e.,  $\mathbf{p} = \lim_{i \rightarrow \infty} B_i$  implies  $f(\mathbf{p}) = \lim_{i \rightarrow \infty} \square f(B_i)$ . For simplicity, we often say “compute  $f(B)$ ” but we actually compute  $\square f(B)$  using interval methods.

**Normalized Taylor Coefficients:** Although IVP theory only requires the function  $f$  in (1) to be locally Lipschitz, practical algorithms need  $f$  to be  $C^k$  for moderately large  $k$ . Following [11], we

assume  $k = 20$  (a global constant) in our implementations. For  $i = 0, \dots, k$ , the  $i$ th **normalized Taylor coefficient** of  $f$  is recursively defined by  $f^{[0]}(\mathbf{x}) = \mathbf{x}$  and for  $i \geq 1$ ,  $f^{[i+1]}(\mathbf{x}) = \frac{1}{i} (J_f^{[i-1]} \bullet f)(\mathbf{x})$  where  $J_f$  is the Jacobian of any  $\mathbf{g} = \mathbf{g}(\mathbf{x}) \in C^1(\mathbb{R}^n \rightarrow \mathbb{R}^n)$ . E.g.,  $f^{[1]} = f$  and  $f^{[2]}(\mathbf{x}) = \frac{1}{2} (J_f \bullet f)(\mathbf{x})$ . The order  $k$  Taylor expansion of  $f(\mathbf{x})$  at the point  $t = t_0$  is

$$\begin{aligned} \mathbf{x}(t_0 + h) &= \left\{ \sum_{i=0}^{k-1} h^i f^{[i]}(\mathbf{x}(t_0)) \right\} + h^k f^{[k]}(\mathbf{x}(\xi)) \\ &\in \left\{ \sum_{i=0}^{k-1} h^i f^{[i]}(\mathbf{x}(t_0)) \right\} + h^k f^{[k]}(F) \end{aligned} \quad (5)$$

where  $0 \leq \xi - t_0 \leq h$  and  $F$  is any enclosure of  $\{\mathbf{x}(t) : t \in [0, h]\}$ .

Since (1) is autonomous, we will normally assume that the initial time is  $t = 0$ . Up to time scaling, we can even make  $h = 1$ . So we can let  $h$  be an optional parameter with default value  $h = 1$ ; this is mainly to simplify notations but our results hold for any  $h > 0$ . Recall the set  $\text{IVP}_f(B_0; h)$  defined in the introduction. If  $B_0 = \{\mathbf{p}_0\}$  is a singleton, we simple write  $\text{IVP}_f(\mathbf{p}_0; h)$ . We say  $\text{IVP}_f(B_0; h)$  is **valid** if for each  $\mathbf{p}_0 \in B_0$ ,  $\text{IVP}_f(\mathbf{p}_0; h)$  is a singleton (comprising the unique solution  $\mathbf{x}$  with  $\mathbf{x}(0) = \mathbf{p}_0$ ). Since  $f$  is usually fixed, they appear in subscripts and is often omitted, as in  $\text{IVP}(B_0; h)$ .

**Admissibility:** The **end set** and **image set** of  $\text{IVP}_f(B_0; h)$  are

$$\begin{aligned} \text{End}_f(B_0; h) &:= \{\mathbf{x}(h) : \mathbf{x} \in \text{IVP}_f(B_0, h)\} \\ \text{Image}_f(B_0, h) &:= \{\mathbf{x}(t) : t \in [0, h], \mathbf{x} \in \text{IVP}_f(B_0, h)\} \end{aligned} \quad (6)$$

Call  $E$  an **end enclosure** of  $\text{IVP}_f(B_0; h)$  if  $E$  contains  $\text{End}_f(B_0; h)$ . Similarly, call  $F$  a **full-enclosure** if  $F$  contains  $\text{Image}_f(B_0; h)$ . Relative to  $f$ , we call  $(B_0, h, F)$  an **admissible triple** and  $(B_0, h, F, E)$  an **admissible quad**. We simply say “admissible” when it is clearly triple or quad. For closed convex sets  $E, F \subseteq \mathbb{R}^n$  and  $h > 0$ , [2, Lemma 1] says that  $(E, h, F)$  is admissible provided and  $E \subseteq \text{interior}(F)$

$$\sum_{i=0}^{k-1} [0, h]^i f^{[i]}(E) + [0, h]^k f^{[k]}(F) \subseteq F. \quad (7)$$

If, in addition, we have  $[0, h]^k f^{[k]}(F) \subseteq [\pm \varepsilon]^n$ , then we say  $(E, h, F)$  is  $\varepsilon$ -**admissible**.

**Logarithmic norms.** Let  $\mu_p(A)$  denote the **logarithmic norm** ( $\log\text{Norm}$ ) of a square matrix  $A \in \mathbb{C}^{n \times n}$  based on the induced matrix  $p$ -norm. For specificity, assume  $p = 2$ . For  $f \in C^1(\mathbb{R}^n \rightarrow \mathbb{R}^n)$ , the **logNorm bound** of  $B \subseteq \mathbb{R}^n$  is defined as  $\mu_2(J_f(B)) := \sup \{\mu_2(J_f(\mathbf{p})) : \mathbf{p} \in B\}$  where  $J_f$  is the Jacobian matrix of  $f$ .

In this paper, in addition to the convention of specifying problems as in the footnote for (3), we have a corresponding header for algorithms that solve the problem:

$$\text{ALGORITHM}(\mathbf{a}; \mathbf{b}; \mathbf{d}) \rightarrow \mathbf{c}. \quad (8)$$

This algorithm header has the problem arguments  $\mathbf{a}; \mathbf{b}$ , but might further have optional “hyperparameters”  $\mathbf{d}$  which have no effect on the correctness of the algorithm, but users can use them to provide hints that may speed up the algorithm.

## 2.2 Review of EndEncl Algorithm

Most validated IVP algorithms are based on two basic subroutines which we call **Step A** and **Step B**, with these headers:

$$\begin{aligned} \text{StepA}_f(E; H = 1) &\rightarrow (h, F) \\ \text{StepB}_f(E, h, F; \varepsilon_0 = w_{\min}(E)) &\rightarrow E_1 \end{aligned} \quad (9)$$

where  $(E, h, F)$  and  $(E, h, F, E_1)$  are admissible. Note that  $H, \varepsilon_0$  are optional, with the indicated default values. Starting with  $E_0$ , we call Step A then Step B to produce an admissible quad:

$$E_0 \xrightarrow{\text{StepA}} (E_0, h_0, F_1) \xrightarrow{\text{StepB}} (E_0, h_0, F_1, E_1). \quad (10)$$

In general, by calling Step A then Step B on  $E_{i-1}$  ( $i = 0, 1, \dots$ ), we produce the the  $i$ th **stage** represented by the admissible quad  $(E_{i-1}, h_i, F_i, E_i)$ . Iterating  $m$  times, we organize these quads into an  **$m$ -stage scaffold** data structure  $\mathcal{S} = (\mathbf{t}, E, F, G)$  where

$$\begin{aligned} \mathbf{t} &= (0 = t_0 < t_1 < \dots < t_m), & E &= (E_0, E_1, \dots, E_m) \\ F &= (F_1, \dots, F_m), & G &= (G_1, \dots, G_m) \end{aligned} \quad (11)$$

where  $t_i = t_{i-1} + h_i$  and the  $G_i$ ’s is the  $i$ th **refinement substructure** that stores data for refining of the  $i$ th stage. This scaffold allows us to achieve much stronger objectives than is possible in the previous IVP algorithms.

Let  $\mathcal{S}$  be an  $m$ -stage scaffold  $\mathcal{S}$ . It is self-modified by 2 subroutines: the first is  $\mathcal{S}.\text{Extend}$ , which turns  $\mathcal{S}$  into a  $m+1$ -stage scaffold. It is straightforward (basically calling Steps A and B), so we focus on the second subroutine with this header:

$\mathcal{S}.\text{Refine}(\varepsilon_0)$   
 INPUT:  $m$ -stage scaffold  $\mathcal{S}$  and  $\varepsilon_0 > 0$ .  
 OUTPUT:  $\mathcal{S}'$  is a refinement of  $\mathcal{S}$  that is  $\varepsilon_0$ -bounded,  
 i.e.,  $w_{\max}(E_m) \leq \varepsilon_0$ .

(12)

Subroutine  $\mathcal{S}.\text{Refine}$  has a while-loop, and each iteration of the while-loop is called a **phase**. Each phase will refine the  $i$ th stage of  $\mathcal{S}$  (from  $i = 1$  to  $i = m$ ). We can visualize each phase as a row of the **phase-stage** diagram in (13):

$$\begin{array}{ccccccccc} & \text{Stage 1} & \cdots & \text{Stage } i & \cdots & \text{Stage } m & & \\ \text{Phase 1:} & \widehat{h}_1^1 & \cdots & \widehat{h}_i^1 & \cdots & \widehat{h}_m^1 & & \\ & \vdots & \vdots & \ddots & \vdots & \ddots & \ddots & \vdots \\ \text{Phase } k: & \widehat{h}_1^k & \cdots & \widehat{h}_i^k & \cdots & \widehat{h}_m^k & & \\ & \vdots & \vdots & \ddots & \vdots & \ddots & \ddots & \vdots \end{array} \quad (13)$$

Each entry of the diagram is indexed by a pair  $(k, i)$  representing the  $k$ th phase at the  $i$ th stage. The operations at  $(k, i)$  are controlled by the  $i$ th refinement substructure

$$G_i = G_i(\mathcal{S}) = ((\pi_i, g_i), (\ell_i, \bar{E}_i, \bar{F}_i), \bar{\mu}_i^1, \bar{\mu}_i^2, \delta_i, h_i^{\text{euler}}). \quad (14)$$

Here we focus on the components in red where  $(\ell_i, \bar{E}_i, \bar{F}_i)$  is the  $i$ th **mini-scaffold** and  $\ell_i \geq 0$  is the **level**. It represents a subdivision of  $[t_i - t_{i-1}]$  into  $2^{\ell_i}$  mini-steps of size  $\widehat{h}_i := (t_i - t_{i-1})2^{-\ell_i}$ , and  $\bar{E}_i, \bar{F}_i$  are  $2^{\ell_i}$ -vectors representing admissible quads  $(\bar{E}_i[j-1], \widehat{h}_i, \bar{F}_i[j], \bar{E}_i[j])$  (for  $j = 1, \dots, 2^{\ell_i}$ ). In (13), we write  $\widehat{h}_i^k$  for the value of  $\widehat{h}_i$  in phase  $k$ . At each  $(k, i)$ , we can refine the  $2^{\ell_i}$  admissible quads by either calling  $\mathcal{S}.\text{EulerTube}(i)$  or  $\mathcal{S}.\text{Bisect}(i)$ . Ideally, we want to call  $\mathcal{S}.\text{EulerTube}(i)$  because it is very fast. But it has a precondition, viz.,  $\widehat{h}_i$  is less than  $h_i^{\text{euler}}$  in  $G_i$  (see (14)). If the precondition fails, we call  $\mathcal{S}.\text{Bisect}(i)$  and also increment the level  $\ell_i$ . This design is critical for the overall performance of our algorithm (see [2, Table B]). The precondition  $\widehat{h}_i < h_i^{\text{euler}}$  guarantees that the polygonal Euler path produced by Euler Tube method is guaranteed to lie in the  $\delta_i$ -tube of each solution  $\mathbf{x} \in \text{IVP}(E_i, t_i - t_{i-1})$  ([2, Lemma 6, Sect.2.5]). The value  $h_i^{\text{euler}}$  is computed by the function  $h^{\text{euler}}(H, \bar{M}, \mu, \delta)$  in [2, Eq. (12)].

### 2.3 Enhanced EndEnc1 Algorithm

We enhance the EndEnc1 algorithm by trying to avoid unnecessary shrinkage of the initial enclosure  $E_0$ . Recall that a **chain** is a sequence

$$C = (1 \leq k(1) \leq k(2) \leq \dots \leq k(m)),$$

such that EulerTube is invoked at phase-stage  $(k(i), i)$  for each  $i$ . It is shown in [2, Appendix A, (H5)] that

$$r_m(C) \leq e^{\bar{\mu}}(r_0(C) + \Delta(C)m) = \underbrace{e^{\bar{\mu}}r_0(C)}_{r_0\text{-part}} + \underbrace{e^{\bar{\mu}}\Delta(C)m}_{\Delta\text{-part}}, \quad (15)$$

where  $r_m(C)$  and  $r_0(C)$  are one half of the maximal widths of the last and first end-enclosures at the corresponding phases, respectively;  $\bar{\mu}$  is the maximal logarithmic norm bound from the first phase; and  $\Delta(C) = \max_{i=1}^m \delta(G_i(\mathcal{S}))$  is evaluated at the initial phase of  $C$ .

```

EndEnc1f( $B_0, \varepsilon_0; \mathbf{p}_0, h$ ) → ( $\underline{B}_0, \bar{B}_1$ )
  INPUT:  $\varepsilon_0 \geq 0$ ,  $h > 0$ , and  $\mathbf{p}_0 \in B_0 \subseteq \mathbb{R}^n$ 
         such that  $\text{IVP}_f(B_0, h)$  is valid
  OUTPUT:  $\underline{B}_0, \bar{B}_1 \in \mathbb{R}^n$ ,  $\mathbf{p}_0 \in \underline{B}_0 \subseteq B_0$ ,  $w_{\max}(\bar{B}_1) < \varepsilon$ 
         and  $\bar{B}_1$  is an end-enclosure of  $\text{IVP}(\underline{B}_0, h)$ .
  _____
   $\mathcal{S} \leftarrow \text{Init}(f, B_0, \varepsilon_0)$   Initialize a 0-stage scaffold
   $t \leftarrow 0$ 
  While  $t < h$ 
     $\mathcal{S}.\text{Extend}(\varepsilon_0, 1-t)$   Extend  $\mathcal{S}$  by one stage
     $\mathcal{S}.\text{Refine}(\varepsilon_0, \mathbf{p}_0)$   Refine  $\mathcal{S}$  until  $w_{\max}(E_{\text{end}}(\mathcal{S})) \leq \varepsilon_0$ 
     $t \leftarrow t(\mathcal{S}).\text{back}()$ 
  Return  $(E_0(\mathcal{S}), E(\mathcal{S}).\text{back}())$ 

```

Note that the optional argument  $\mathbf{p}_0$  is passed to  $\mathcal{S}.\text{Refine}(\varepsilon_0, \mathbf{p}_0)$ ; In the Refine of [2],  $E_0(\mathcal{S})$  is updated by the simple line

$$E_0(\mathcal{S}) \leftarrow \frac{1}{2}E_0(\mathcal{S}) \quad (16)$$

to halve  $E_0(\mathcal{S})$  at the end of the while-loop. We now shrink  $E_0(\mathcal{S})$  conditionally, as indicated by the line in green. Moreover, we shrink  $E_0(\mathcal{S})$  toward the point  $\mathbf{p}_0$ ; the shrinkage step (16) is now

$$E_0(\mathcal{S}) \leftarrow \mathbf{p}_0 + \frac{1}{2}(E_0 - \mathbf{p}_0). \quad (17)$$

Note that " $E_0 - \mathbf{p}_0$ " translates  $E_0$  so that  $\mathbf{p}_0$  becomes the origin; after halving  $\frac{1}{2}(E_0 - \mathbf{p}_0)$ , we translate the origin of  $\frac{1}{2}(E_0 - \mathbf{p}_0)$  back to  $\mathbf{p}_0$ .

For a given chain  $C$ , if  $2r_m(C) < \varepsilon_0$  then the Refine procedure halts. Hence, by (15), Refine will terminate as soon as both the  $r_0$ -part and the  $\Delta$ -part are bounded by  $\varepsilon_0/4$ ; i.e., when

$$e^{\bar{\mu}}r_0(C) < \frac{\varepsilon_0}{4} \quad \text{and} \quad e^{\bar{\mu}}\Delta(C)m < \frac{\varepsilon_0}{4}. \quad (18)$$

Therefore, to simplify the subsequent complexity analysis of Refine (without affecting termination), we modify Refine by imposing the following stopping rules:

1. If

$$\frac{1}{2}w_{\max}(E_0(\mathcal{S}))e^{\bar{\mu}} < \varepsilon_0/4, \quad (19)$$

then  $E_0(\mathcal{S})$  is no longer shrunk.

2. For each  $i = 1, \dots, m$ , if

$$e^{\bar{\mu}}\delta(G_i(\mathcal{S}))m < \varepsilon_0/8, \quad (20)$$

then we do nothing for this stage.

3. In each phase, let  $\Delta := \max_{i=1}^m \delta(G_i(\mathcal{S}))$ . If

$$e^{\bar{\mu}}\Delta m < \varepsilon_0/8, \quad \text{and condition 1 (19): } \frac{1}{2}w_{\max}(E_0(\mathcal{S}))e^{\bar{\mu}} < \varepsilon_0/4$$

then for each stage we double the value of  $\delta(G_i(\mathcal{S}))$  and invoke EulerTube for to produce a chain  $C$  and stop the Refine algorithm.

Note that in Condition (20) we require  $< \varepsilon_0/8$ , rather than  $< \varepsilon_0/4$  as in (18). This is because in  $\mathcal{S}.\text{Refine}$  we always call EulerTube first and then halve  $\delta$ . Consequently, when Condition 2 is detected to hold, the corresponding stage has just used twice the current value of  $\delta$  and invoked EulerTube.

Since stages satisfying Condition 2 are skipped, and Condition 3 requires that *every* stage satisfy Condition 2, let  $\Delta := \max_{i=1}^m \delta(G_i(\mathcal{S}))$ . The requirement of Condition 3 can then be written as  $e^{\bar{\mu}}\Delta m < \varepsilon_0/8$ , which implies that all stages are in the state obtained after calling EulerTube with the doubled  $\delta$ . Therefore, doubling the values  $\delta(G_i(\mathcal{S}))$  and invoking EulerTube for every stage produces a new chain that satisfies (18).

```

S.Refine( $\varepsilon_0, \mathbf{p}_0$ )
  INPUT:  $m$ -stage scaffold  $\mathcal{S}$  and  $\varepsilon_0 > 0$ , a point  $\mathbf{p}_0 \in E_0(\mathcal{S})$ .
  OUTPUT:  $\mathcal{S}$  remains an  $m$ -stage scaffold
         that satisfies  $w_{\max}(E_m) \leq \varepsilon_0$ .
  _____
   $r_0 \leftarrow w_{\max}(E_m(\mathcal{S}))$ .
  While  $(r_0 > \varepsilon_0)$ 
    ▷ The original code, " $E_0(\mathcal{S}) \leftarrow \frac{1}{2}E_0(\mathcal{S})$ ," is replaced by the next lines:
     $\bar{\mu} \leftarrow \max\{\bar{\mu}^i(G_i(\mathcal{S})): i = 1, \dots, m\}$ .
     $\Delta \leftarrow \max_{i=1}^m (\delta(G_i(\mathcal{S})))$ .
    If  $(e^{\bar{\mu}}\Delta m < \varepsilon_0/8 \text{ and } e^{\bar{\mu}}(t_m(\mathcal{S}) - t_0(\mathcal{S})) w_{\max}(E_0(\mathcal{S})) < \varepsilon_0/2)$ 
      For  $(i = 1, \dots, m)$   Condition 3 is satisfied
         $G_i(\mathcal{S}).\delta \leftarrow 2G_i(\mathcal{S}).\delta$ 
        S.EulerTube( $i$ ).  Create a chain
      Return  $\mathcal{S}$   Stop the algorithm
     $r_0 \leftarrow w_{\max}(E_m(\mathcal{S}))$ 
    For  $(i = 1, \dots, m)$   Begin new phase
      If  $(e^{\bar{\mu}}\delta(G_i(\mathcal{S}))m < \varepsilon_0/8)$   Condition 2 (20)
        Continue  Skip this stage
      Let  $\ell \leftarrow G_i(\mathcal{S}).\ell$  and  $\Delta t_i \leftarrow t(\mathcal{S}).t_i - t(\mathcal{S}).t_{i-1}$ .
       $H \leftarrow (At_i)^2$ .
      If  $(H > \hat{h})$ 
        S.Bisect( $i$ )
      Else
        S.EulerTube( $i$ )
      Let  $G_i(\mathcal{S})$  be  $(\pi, \mathbf{g}, \bar{\mu}^1, \bar{\mu}^2, \delta, \hat{h}, (\ell, E, F))$  after the Euler Tube.
      ▷ We must update  $\delta$  and  $\hat{h}$  for the next Euler Tube event.
       $G_i(\mathcal{S}).\delta \leftarrow \delta/2$   (Updating the  $\delta$  target is easy)
      ▷ Updating  $\hat{h}$  to reflect the  $\delta$  requires six preparatory steps: (1)-(6)
      (1)  $E_i(\mathcal{S}) \leftarrow E[2^\ell]$   End-enclosure for stage
      (2)  $F_i(\mathcal{S}) \leftarrow \bigcup_{j=1}^{2^\ell} F[j]$   Full-enclosure for stage
      (3)  $\mu_2^2 \leftarrow \max\{\bar{\mu}^j[j]: j = 1, \dots, 2^\ell\}$ 
      (4)  $\hat{\delta}_1^j \leftarrow \text{TransformBound}(\delta, \pi, F_i(\mathcal{S}))$ 
      (5)  $\hat{M} \leftarrow \|\mathbf{g}^{[2]}(\pi(F_i(\mathcal{S})))\|_2$ 
      (6)  $h_{\text{tmp}} \leftarrow \min\{\Delta t_i, h_{\text{euler}}(\hat{h}, \hat{M}, \mu_2^2, \delta_1^j)\}$ 
       $G_i(\mathcal{S}).\hat{h} \leftarrow h_{\text{tmp}}$   Finally, update  $\hat{h}$ 
    ▷ End of For-Loop
    ▷ The original code, " $E_0(\mathcal{S}) \leftarrow \frac{1}{2}E_0(\mathcal{S})$ ," is replaced by the next lines:
    If  $e^{\bar{\mu}}(t_m(\mathcal{S}) - t_0(\mathcal{S})) w_{\max}(E_0(\mathcal{S})) > \varepsilon_0/2$   Condition 1 (19)
       $E_0(\mathcal{S}) \leftarrow \mathbf{p}_0 + \frac{1}{2}(E_0(\mathcal{S}) - \mathbf{p}_0)$ 
     $r_0 \leftarrow w_{\max}(E_m(\mathcal{S}))$ 
  ▷ End of While-Loop
  Return  $\mathcal{S}$ 

```

### 2.4 The End Cover Algorithm

Let  $B \in \mathbb{R}^n$  be a box. If  $\text{IVP}_f(B, H)$  is valid, then the bundle  $\Phi = \Phi f(B, H)$  exists by Theorem 3.

It follows from Theorem 4 that we can construct an  $\varepsilon$ -cover for  $\Phi$  by calling EndEnc1 to generate a sequence of box pairs  $(\underline{B}_i, \bar{B}_i)$ . For the given initial box  $B_0$ , if  $B_0 \subseteq \bigcup_{i=1}^m \underline{B}_i$ , then the union of the  $\bar{B}_i$ ,namely  $\bar{B}_1 := \bigcup_{i=1}^m \bar{B}_i$ , constitutes a valid enclosure; in other words,  $\text{EndCover}_f(B_0, \varepsilon) \rightarrow \bar{B}_1$ .

$\text{EndCover}_f(B_0, \varepsilon, H) \rightarrow \bar{B}_1$

INPUT:  $B_0 \subseteq \mathbb{R}^n$ ,  $\varepsilon > 0$ ,  $H > 0$ .

OUTPUT:  $\bar{B}_1 \subseteq \mathbb{R}^n$  satisfying

$$\text{End}_f(B_0, h) \subseteq \bar{B}_1 \subseteq (\text{End}_f(B_0, h) \oplus [\pm \varepsilon]^n).$$

$$S_0 \leftarrow \{B_0\}, S \leftarrow \emptyset, P \leftarrow \emptyset$$

While  $S_0 \neq \emptyset$

$$\text{Let } B.\text{pop}(S_0) = \prod_{i=1}^n [a_i, b_i]$$

$$\mathbf{p} = \text{mid}(B) \quad \text{a Midpoint of } B$$

$$(\underline{B}, \bar{B}) \leftarrow \text{EndEnc1}(B, \varepsilon; \mathbf{p}, H)$$

If  $(\underline{B} \neq B)$

$$I_i^{k_i} := \left[ a_i + \frac{k_i}{2}(b_i - a_i), a_i + \frac{k_i+1}{2}(b_i - a_i) \right]$$

$$S_0 \leftarrow S_0 \cup \left\{ \prod_{i=1}^n I_i^{k_i} : k_i \in \{0, 1\} \right\}.$$

$$S \leftarrow S \cup \bar{B}.$$

Return  $S$ .

### 3 Boundary Cover Problem

We now consider another approach to the End Cover Problem, by reducing it to a lower dimensional problem called **Boundary Cover Problem**. First, we provide the theoretical justification.

#### 3.1 Trajectory Bundles

We now use a more geometric language and call each  $\mathbf{x} \in \text{IVP}_f(\mathbf{p}_0, h)$  a trajectory. The classic theorem of Picard-Lindelöf [12, 13] gives conditions for the existence and uniqueness of trajectories in  $\text{IVP}_f(\mathbf{p}_0, h)$  for a point  $\mathbf{p}_0$ . But these proofs actually show much more as we now show.

A **trajectory** with **time-span**  $[0, h]$  is a  $C^1$ -function of the form  $\phi : [0, h] \rightarrow \mathbb{R}^n$ . Moreover,  $\phi$  is a  **$f$ -trajectory** if  $\phi \in \text{IVP}(B, h)$  for some  $B \subseteq \mathbb{R}^n$  (i.e.,  $\phi'(t) = f(\phi(t))$  and  $\phi(0) \in B$ ). Call

$$\Phi : [0, h] \times B \rightarrow \mathbb{R}^n \quad (21)$$

a **trajectory bundle** if  $\Phi(\tau, \mathbf{p})$  is a continuous function on  $[0, h] \times B$  such that  $\Phi(0, \mathbf{p}) = \mathbf{p}$  (for all  $\mathbf{p} \in B$ ) and satisfies the following **stratification property**:

$$(\forall \mathbf{p} \neq \mathbf{q} \in B) (\forall \tau \in [0, h]) \quad [\Phi(\tau, \mathbf{p}) \neq \Phi(\tau, \mathbf{q})]. \quad (22)$$

For all  $\tau \in [0, h]$ ,  $\mathbf{p} \in B$ , we have the induced functions  $\Phi|_{\mathbf{p}}$  and  $\Phi|^{\tau}$

$$\left. \begin{array}{l} \Phi|_{\mathbf{p}} : [0, h] \rightarrow \mathbb{R}^n \quad (\mathbf{p}\text{-trajectory}), \\ \Phi|^{\tau} : B \rightarrow \mathbb{R}^n \quad (\tau\text{-end map}). \end{array} \right\} \quad (23)$$

where  $\Phi|_{\mathbf{p}}(\tau) = \Phi|^{\tau}(\mathbf{p}) = \Phi(\tau, \mathbf{p})$ . Call  $\Phi$  a  **$f$ -bundle** on  $(B, h)$ . If each  $\Phi|_{\mathbf{p}}$  is a  $f$ -trajectory ( $\mathbf{p} \in B$ ), then denote this bundle by  $\Phi = \Phi_{f, B, h}$ . The stratification property (22) says that the graphs of the trajectories  $\Phi|_{\mathbf{p}}$  and  $\Phi|_{\mathbf{q}}$  for  $\mathbf{p} \neq \mathbf{q}$  are pairwise disjoint. We can now re-state the Picard-Lindelöf Theorem in terms of trajectory bundles:

**THEOREM 1 (PICARD-LINDELÖF).**

Let  $f : \mathbb{R}^n \rightarrow \mathbb{R}^n$  be locally Lipschitz.

For all  $\mathbf{p}_0 \in \mathbb{R}^n$ , there exists  $h, r > 0$  such that there exists an  $f$ -bundle

$$\Phi : [0, h] \times \text{Ball}_{\mathbf{p}_0}(r) \rightarrow \mathbb{R}^n$$

This bundle formulation is natural for applications since one is seldom interested in a single trajectory, but in an entire bundle. Moreover, Picard-Lindelöf only guarantees existence and uniqueness in some small enough time span  $[0, h]$ . To cover a time span  $[0, H]$  ( $H > h$ ) we need to patch together such bundles over time spans  $[t_i, t_i + h_i]$  ( $i = 1, \dots, N$ ) that cover  $[0, H]$ . The next theorem is such an application. Define  $\text{Valid}_f(H)$  to be the set of all points  $\mathbf{p} \in \mathbb{R}^n$  such that  $\text{IVP}_f(\mathbf{p}, H)$  is valid.

**THEOREM 2.** The set  $\text{Valid}_f(H)$  is an open set for any  $H > 0$ .

This theorem is trivial when  $\text{Valid}_f(H)$  is empty since empty sets are open.

**THEOREM 3 (EXISTENCE OF  $f$ -BUNDLES).** If  $f : \mathbb{R}^n \rightarrow \mathbb{R}^n$  is locally Lipschitz, and  $B \subseteq \text{Valid}_f(H)$ , then the  $f$ -bundle  $\Phi_f(B, H)$  exists.

**The End Slice Map  $\text{End}_f$ :** If  $\Phi$  is the trajectory bundle in (21), the  $\tau$ -slice (for  $\tau \in [0, h]$ ) of  $\Phi$  is the set

$$\Phi|^{\tau} := \{\Phi(\tau, \mathbf{p}) : \mathbf{p} \in B\}. \quad (24)$$

E.g., the 0-slice is just  $B$ . The  $h$ -slice  $\Phi|^h$  is called the **end-slice**. Define the **end map** of  $\Phi$  to be

$$\text{End}_{\Phi} : B \rightarrow \mathbb{R}^n \quad (25)$$

where  $\text{End}_{\Phi}(\mathbf{p}) = \Phi(h, \mathbf{p})$ .

**THEOREM 4.** Let  $\Phi : [0, h] \times B \rightarrow \mathbb{R}^n$  be a trajectory bundle where  $B \in \mathbb{R}^n$ . Then the end map  $\text{End}_{\Phi}$  of (25) is a homeomorphism from  $B$  onto the end-slice  $\Phi|^h$ .

Note that our theorem holds even when  $\dim(B) < n$ ; we need this generality in our boundary technique below. The proof of this theorem depends on a famous result of L.E.J. Brouwer (1912):

**PROPOSITION 5. Brouwer's Invariance of Domain**

If  $U$  is an open set in  $\mathbb{R}^n$  and  $f : U \rightarrow \mathbb{R}^n$  is continuous and injective, then  $f(U)$  is also open. In particular,  $U$  and  $f(U)$  are homeomorphic.

#### 3.2 Reduction of End Cover to Boundary Cover

Theorem 4 justifies the following **Boundary Algorithm** for computing an  $\varepsilon$ -box cover of  $\text{End}_f(B, h)$ : if  $B \in \mathbb{R}^n$ , we compute an  $\varepsilon$ -box cover  $C_i$  ( $i = 1, \dots, 2n$ ) for each of the  $2n$  faces of  $B$ . Then

$$\bar{C} := \bigcup_{i=1}^{2n} C_i$$

is an  $\varepsilon$ -box cover for the boundary  $\partial(\text{End}_f(B, h))$ . Next, we compute a **filler cover**  $C_0$  to cover the “interior” of  $\bar{C}$  so that  $\bar{C} \cup C_0$  forms an  $\varepsilon$ -box cover of  $\text{End}_f(B, h)$ .

Thus, the Boundary Algorithm reduces an  $n$ -dimensional cover problem to several  $(n-1)$ -dimensional ones, modulo the **Fill Problem** of computing  $C_0$ ; the header for this problem is thus

$$\text{Filler}(\bar{C}, \varepsilon) \rightarrow C_0$$

Unfortunately, this appears to be an ill-formed problem unless  $\varepsilon$  is small enough. To understand the difficulty, note that  $\cup \bar{C}$  is a connected set. The boundary of  $\cup \bar{C}$  is the union of finitely many components,  $S_0 \cup S_1 \cup \dots \cup S_k$  where each  $S_j$  is topologically an  $(n-1)$ -sphere. Moreover,  $S_0$  is the unique exterior component such that the other  $S_i$ 's ( $i = 1, \dots, k$ ) lies in the interior of  $S_0$ . Also the  $S_i$ 's are not nested (if  $S_i$  is contained in some  $S_j$  then  $j = 0$ ).

We want the filler set  $C_0$  to lie inside  $S_0$ , and to cover up *some* of these  $S_i$ 's. But identifying the  $S_i$ 's to cover is a non-trivial problem especially in higher dimensions. Let us say that  $\varepsilon$  is **small enough** if  $k = 1$ . If  $\varepsilon$  is small enough, then the boundary  $\partial(\bigcup \bar{C})$  has two components  $S_0, S_1$  with  $S_1$  inside  $S_0$ . The boxes of  $C_0$  just have to cover the interior of  $S_1$  but stay within  $S_0$ . This is a relatively simpler problem of computational geometry, with no need for any IVP solving. In our examples ( $n = 2$ ), we can visually see that our  $\varepsilon$  is small enough. In our experimental section, we will compare this Boundary Algorithm with  $\text{EndCover}_f(B_0, \varepsilon)$ .

## 4 Complexity Analysis

In this section, we provide a detailed analysis of the computational complexity of the proposed EndCover algorithm. Since EndCover relies heavily on EndEnc1 as its primary subroutine, we start by dissecting the complexity of EndEnc1 to build a foundational understanding before addressing the overall framework.

### 4.1 Complexity of End Enclosure Algorithm

To gain insight into the performance of EndEnc1, we break down its complexity into three key components:

- (1) The total number of calls to Extend and Refine, that is, the number of stages generated by the EndEnc algorithm;
- (2) The computational complexity of a single call to Extend;
- (3) The computational complexity of a single call to Refine.

To facilitate the complexity analysis, we recall the following notation from [2, Lemma 6]. For given  $(E_0, H, \varepsilon > 0)$  we define

$$\bar{B}(E_0, H, \varepsilon) := \sum_{i=0}^{k-1} [0, H]^i f^{[i]}(E_0) + \text{Box}(\varepsilon), \quad (26)$$

$$\bar{h}(E_0, H, \varepsilon) := \min \left\{ H, \min_{i=1}^n \left( \frac{\varepsilon_i}{M_i} \right)^{1/k} \right\}, \quad (27)$$

where

$$M_i := \sup_{p \in \bar{B}(E_0, H, \varepsilon)} \left| (f^{[k]}(p))_i \right|, \quad (i = 1, \dots, n), \quad (28)$$

and  $(\mathbf{x})_i$  denotes the  $i$ th coordinate function.

**4.1.1 Upper bound on the number of stages.** We begin by establishing an upper bound on the total number of stages produced by the EndEnc algorithm. This bound is essential as it limits the depth of the iterative process and directly influences the overall complexity. The following lemma quantifies this aspect:

LEMMA 6.

The number of stages in  $\text{EndEnc1}(E_0, \varepsilon; \mathbf{p}, H)$  is at most  $1 + \lfloor H/\bar{h} \rfloor$  where  $\bar{h} = \bar{h}(\bar{E}, H, \varepsilon)$ , see (27) and  $\bar{E} = \text{image}(\text{IVP}(E_0, H)) + \text{Box}(\varepsilon)$ .

This result highlights how the parameters  $H$  and  $\bar{h}$  govern the progression of stages, ensuring the algorithm does not extend indefinitely.

**4.1.2 Complexity of the Extend Subroutine.** The Extend subroutine advances the scaffold by appending a new stage. This is accomplished through calls to StepA and StepB, together with a small number of auxiliary operations, in order to construct admissible triples and validated enclosures. From the perspective of complexity analysis, the overall cost of Extend is dominated by the behavior

of StepA, since it determines the number of iterations required to obtain an admissible extension. The remaining operations are loop-free and involve only constant-time computations; for example, a call to StepB mainly performs Taylor expansions of order  $k$  for an  $n$ -dimensional system.

LEMMA 7. *Given a scaffold  $\mathcal{S}$  with  $m$  stages and parameters  $\varepsilon > 0$  and  $H > 0$ , the subroutine StepA executed within  $\mathcal{S}.\text{Extend}(\varepsilon, H)$  performs at most*

$$\left\lceil \log_2 \left( \frac{H}{\bar{h}} \right) \right\rceil$$

*internal iterations, where  $\bar{h} = \bar{h}(E_m(\mathcal{S}), H, \varepsilon)$  is defined in (27).*

**4.1.3 Complexity of Refine subroutine.** Before delving into the complexity, it is important to confirm that the modified Refine subroutine reaches a termination point, ensuring the algorithm's reliability:

LEMMA 8. *The modified Refine subroutine terminates.*

With termination established, we proceed to quantify the computational complexity of the Refine algorithm. This involves considering the contributions from multiple phases and the parameters that influence refinement steps:

LEMMA 9. *Let  $\mathcal{S}$  be an  $m$ -stage scaffold, and let  $\varepsilon_0 > 0$ . For each stage  $i$  write  $\Delta t_i = t_{i+1}(\mathcal{S}) - t_i(\mathcal{S})$  and*

$$G_i(\mathcal{S}) = (\pi_i, \mathbf{g}_i, \bar{\mu}_i^1, \bar{\mu}_i^2, \delta_i, \bar{h}_i, (\ell_i, E_i, F_i)).$$

*Let  $I_i = [a, b]$  be an interval satisfies:*

$$a = \min_{\mathbf{q} \in \pi(F_i(\mathcal{S}))} (\mu_2(J_{\mathbf{g}_i}(\mathbf{q}))) \quad \text{and} \quad b = \max_{i=1, \dots, m} (\max \bar{\mu}_i^2).$$

*Let*

$$\bar{\mu} = \max_{i=1, \dots, m} (\max \bar{\mu}_i^1), \quad \Delta_{\max} = \max_{i=1, \dots, m} \delta_i, \quad M_i = \|\mathbf{g}_i^{[2]}(\pi(F_i(\mathcal{S})))\|_2,$$

$$\text{and define } \delta'_i = \text{TransformBound} \left( \min \left( \delta_i, \frac{\varepsilon_0}{16m\bar{\mu}} \right), \pi, F_i(\mathcal{S}) \right),$$

$$N = \left\lceil \max_{i=1, \dots, m, p \in I_i} \left( \log_2 \left( \frac{\Delta t_i}{h^{\text{euler}}(\Delta t_i, M_i, p, \delta'_i)} \right) \right) \right\rceil. \quad (29)$$

*Then the number of phases in  $\mathcal{S}.\text{Refine}(\varepsilon_0)$  is at most*

$$1 + \max \left\{ \left\lceil \log_2 \frac{2 w_{\max}(E_0(\mathcal{S})) e^{\bar{\mu}}}{\varepsilon_0} \right\rceil, \left\lceil \log_2 \frac{8m \Delta_{\max} e^{\bar{\mu}}}{\varepsilon_0} \right\rceil + N \right\}.$$

## 4.2 Complexity of End Cover Algorithm

Building upon the analysis of EndEnc1, we now turn our attention to the overarching complexity of the EndCover algorithm. This higher-level procedure orchestrates multiple calls to EndEnc1, and understanding its complexity requires integrating the insights from the subroutine analyses.

From Lemma 6, each invocation of EndEnc1 generates at most  $1 + \lfloor H/\bar{h} \rfloor$  stages. Furthermore, within each stage, the Refine subroutine is called exactly once, and its complexity is bounded as per Lemma 9. These elements combine to yield the complexity of individual EndEnc1 calls.

To complete the picture, we must bound the number of times EndCover invokes EndEnc1. The following theorem addresses this:

**THEOREM 10.** Let  $\bar{B} = \text{image}(\text{IVP}(B_0, H)) + \text{Box}(\varepsilon)$  and  $\bar{\mu} = \mu_2(J(f(\bar{B})))$ . Then  $\text{EndCover}(B_0, H, \varepsilon)$  will call  $\text{EndEnc1}$  at most

$$\Theta\left(\left(\frac{2w_{\max}(B_0)e^{\bar{\mu}}}{\varepsilon}\right)^n\right)$$

times.

## 5 Experiments

In this section, we provide a detailed analysis of the computational complexity of the proposed  $\text{EndCover}$  algorithm. Since  $\text{EndCover}$  relies heavily on  $\text{EndEnc1}$  as its primary subroutine, we start by dissecting the complexity of  $\text{EndEnc1}$  to build a foundational understanding before addressing the overall framework.

### 5.1 Experiments

In this section, we present empirical evaluations to demonstrate the practical efficacy and advantages of our proposed method. Our experiments are based on the models given in Table 1.

To provide a concrete illustration, we begin with a detailed example that highlights the key features and benefits of our approach in action.

**EXAMPLE 1.** Consider the Volterra system

$$\begin{cases} x' = 2x - 2xy, \\ y' = -y + xy, \end{cases}$$

with initial box  $B_0 = [0.9, 1.1] \times [2.9, 3.1]$ . We compute the end-enclosures of the four edges of  $B_0$  at final time  $T = 1$ . The four resulting enclosures are:

- Edge 1:  $[0.0590893, 0.0912428] \times [1.36636, 1.49452]$ ,
- Edge 2:  $[0.0605758, 0.0970096] \times [1.42774, 1.56825]$ ,
- Edge 3:  $[0.0686275, 0.10654] \times [1.38487, 1.48567]$ ,
- Edge 4:  $[0.0534886, 0.083121] \times [1.44681, 1.54128]$ .

The smallest box enclosing all four edge enclosures (i.e., their wrapping) is:

$$[0.0534886, 0.10654] \times [1.36636, 1.56825].$$

In contrast, a direct enclosure computed for the entire box  $B_0$  (without decomposition) yields:

$$[0.0168262, 0.137862] \times [1.30876, 1.62013].$$

This comparison underscores the key strength of our boundary-based propagation strategy. By decomposing the problem into edge-specific evolutions and subsequently combining the results, we achieve a much tighter end-enclosure. Quantitatively, the area of our method's enclosure is approximately 3.52 times smaller than that of the direct approach, illustrating how our technique mitigates the wrapping effect and delivers sharper, more precise bounds that are invaluable for reliable uncertainty quantification in dynamical systems.

The figures below illustrate the trajectories produced by our method and demonstrate how the corresponding end enclosures are obtained.

From these figures, we observe that, in contrast to Lohner's method, our approach mitigates the wrapping effect by explicitly

tracking and propagating the boundary of the reachable set. This boundary-oriented strategy prevents excessive over-approximation during enclosure propagation, which explains why our method is able to produce significantly tighter and more accurate end enclosures.

To further substantiate the performance of our algorithm,

We conducted a series of comparative experiments against three established interval-based IVP solvers. Here, "Ours" denotes our  $\text{EndCover\_Algo}$ . The baseline includes  $\text{StepB}_{\text{Direct}}$ , a traditional iterative scheme that alternates between  $\text{stepA}$  and  $\text{stepB}$ , with  $\text{stepB}$  utilizing the direct method. Additionally, "VNODE-LP" and "CAPD" represent the Lohner [8] and Cr-Lohner [19] methods, respectively, with a parameter setting of  $(r = 3)$ . All methods were tasked with computing the end-enclosure for  $(\text{IVP}(B_0, T))$  under identical conditions.

Note that the output of our method is a collection of boxes whose union constitutes the  $\varepsilon$ -bounded end cover. To enable a direct comparison with other approaches, we replace this collection by its minimal enclosing box. As a consequence, the reported enclosure is a strict over-approximation of the true output. But results reported in Table 2 demonstrate that our algorithm consistently outperforms the competing methods in terms of both enclosure tightness and numerical robustness. For almost all test cases, our method produces the smallest enclosures, and the performance gap becomes more pronounced as the time horizon  $T$  increases, see  $\frac{w_{\max}(\text{others})}{w_{\max}(\text{ours})}$  column.

It is worth noting that VNODE-LP and CAPD can compute enclosures efficiently for small integration times  $T$ . However, as  $T$  increases these enclosures tend to grow rapidly; consequently some computations—most notably the QR decompositions used in Lohner-type procedures—can become numerically unstable and the method may fail to produce results (see Eg1, Eg2, Eg4). It is unclear whether more stable version of CAPD exists. However, the experimental data for Example 1 at  $(T = 2, 4, 5.5)$  indicate that the ratio  $w_{\max}(\text{CAPD})/w_{\max}(\text{ours})$  at  $T = 5.5$  if a result can be produced, is expected to be larger than its value at  $T = 4$ .

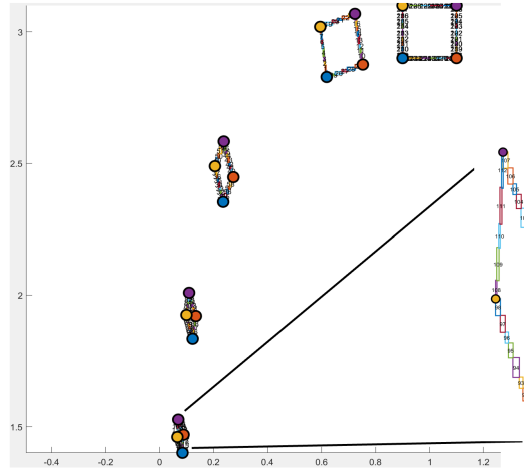
Classical iterative interval method is further affected by the wrapping effect: enclosures tend to inflate over time, forcing the step size to decrease rapidly. This behavior significantly increases the computational cost and, in many cases, prevents the computation from completing.

In contrast, our boundary cover method avoids the wrapping effect by explicitly tracking the boundary of the enclosure, rather than relying on matrix factorization. This design leads to improved numerical stability. Furthermore, the algorithm repeatedly invokes  $\text{Refine}$  during the integration process, preventing intermediate enclosures from becoming excessively large and thereby avoiding unnecessary step-size reductions. When  $T$  is small, the Boundary cover method is not as fast as the End cover method. This is because the End cover method requires only a small number of subdivisions, whereas the Boundary cover method must process each face of the enclosure. For larger values of  $T$ , however, the advantage of the Boundary cover becomes apparent, since it only needs to handle the boundary of the reachable set; see Examples Eg1, Eg2, Eg5.

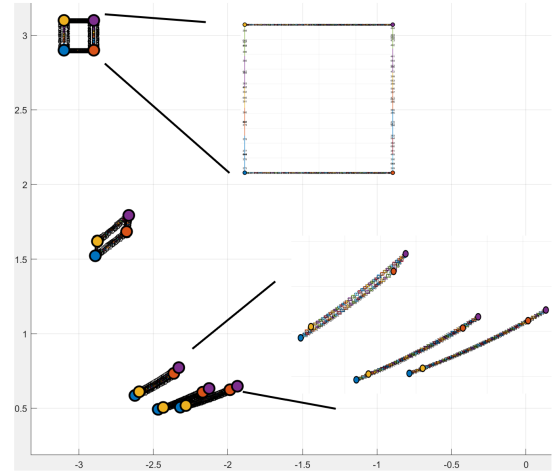
To further analyze the impact of the tolerance parameter  $\varepsilon$  on algorithm performance, we tested our method under different  $\varepsilon$

Eg*	Name	$f(x)$	Parameters	Box $B_0$	Reference
Eg1	Lottka-Volterra Predator-Prey	$(-ax(1-y), -by(1-x))$	$(a, b) = (2, 1)$	$Box_{(1,3)}(0.1)$	[14], [15, p.13]
Eg2	Van der Pol	$(y, -c(1-x^2)y - x)$	$c = 1$	$Box_{(-3,3)}(0.1)$	[15, p.2]
Eg3	Asymptote	$(x^2, -y^2 + 7x)$	N/A	$Box_{(-1.5,8.5)}(0.01)$	N/A
Eg4	Quadratic	$(y, x^2)$	N/A	$Box_{(1,-1)}(0.05)$	[15, p.11]
Eg5	FitzHugh-Nagumo	$(x - \frac{x^3}{3} - y + I, \epsilon(x + a - by))$	$(a, b, \epsilon, I) = (0.7, 0.8, 0.08, 0.5)$	$Box_{(1,0)}(0.1)$	[16]
Eg6	Reduced Robertson (2D)	$(-k_1 x + k_2 y(1-x-y), k_1 x - k_2 y(1-x-y) - k_3 y^2)$	$(k_1, k_2, k_3) = (0.04, 10^4, 3 \times 10^7)$	$Box_{(1,0)}(10^{-6})$	[17]
Eg7	Lorenz	$(\sigma(y-x), x(\rho-z) - y, xy - \beta z)$	$(\sigma, \rho, \beta) = (10, 28, 8/3)$	$Box_{(15,15,36)}(0.001)$	[15, p.11]
Eg8	Rossler	$(-y - z, x + ay, b + z(x - c))$	$(a, n, c) = (0.2, 0.2, 5.7)$	$Box_{(1,2,3)}(0.1)$	[18]

Table 1: List of IVP Problems



(a) Eg1: Results at  $(T = 0, 0.1, 0.4, 0.7, 1.0)$ . An enlarged view at  $(T = 0.0, 1.0)$  is also shown.



(b) Eg2: Results at  $(T = 0, 0.1, 0.4, 0.7, 1.0)$ . An enlarged view at  $(T = 0.4, 0.7, 1.0)$  is also shown.

Figure 3: Trajectories and end enclosures for Examples Eg1 and Eg2 with  $\epsilon = 0.01$ .

values. Table 3 records how the interval width and computation time vary with  $\epsilon$ .

**Experimental Conclusion Summary:** Table 3 shows that decreasing the tolerance parameter  $\epsilon$  generally leads to contraction of interval widths (e.g.,  $w_{\max}$  decreases from 0.20 to 0.12 in Eg1), but at the cost of increased computation time. Notably, when  $\epsilon$  falls below a certain threshold (e.g.,  $\epsilon \leq 0.1$  in Eg2 and Eg3), the interval width no longer changes significantly, indicating that the algorithm has reached its precision limit. This phenomenon provides guidance for selecting appropriate  $\epsilon$  values in practical applications: excessively small  $\epsilon$  may unnecessarily increase computational costs without improving accuracy.

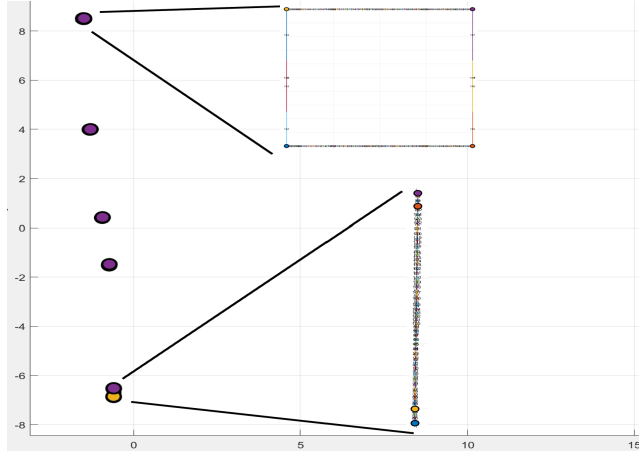
Table 4 summarizes how the output enclosure and computational effort depend on the time horizon  $T$ . In general, increasing  $T$  tends to enlarge the computed enclosure and to increase the number of initial boxes  $\#(B_0)$  and run time. The effect can be mild for some problems (e.g., the Quadratic example shows only modest changes in time and  $\#(B_0)$ ), but can be drastic for others: Eg2 at  $T = 4.0$  requires 56 initial boxes and about 20.36 s, whereas at  $T \leq 2.0$  it used at most 10 boxes and under 0.31 s. This indicates that long time propagation may require significantly more subdivision and thus higher computational cost;

## 6 Conclusion

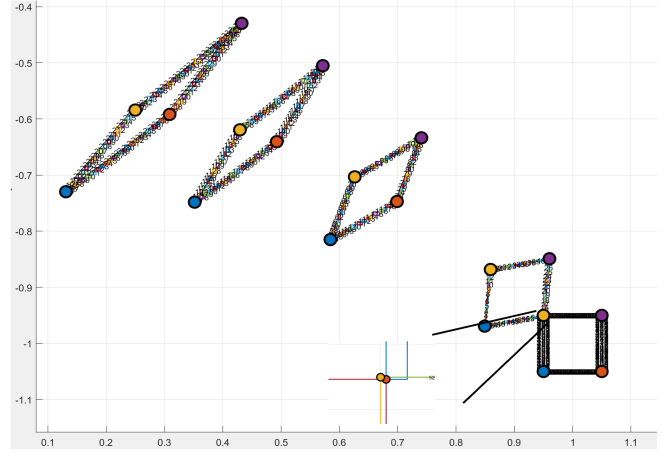
We have designed a complete validated algorithm for a variant of the IVP problem, called the End Cover Problem. We also offer an alternative technique based on covering the boundary of the End Cover that provides tighter enclosures. Preliminary implementations show that our algorithms are practical and outperforms existing validated algorithms (CAPD and VNODE-LP).

## References

- [1] Ramon E. Moore. *Interval Analysis*. Prentice Hall, Englewood Cliffs, NJ, 1966.
- [2] Bingwei Zhang and Chee Yap. A Novel Approach to the Initial Value Problem with a Complete Validated Algorithm. *arXiv preprint arXiv:2502.00503*, February 2025.
- [3] G. F. Corliss. Survey of interval algorithms for ordinary differential equations. *Appl.Math.Comp.*, 31, 1989.
- [4] Kai Shen, Dillard L. Robertson, and Joseph K. Scott. Tight reachability bounds for constrained nonlinear systems using mean value differential inequalities. *Automatica*, 134:109911, 2021.
- [5] Chuchu Fan, Kristina Miller, and Sayan Mitra. Fast and guaranteed safe controller synthesis for nonlinear vehicle models. In Shuvendu K. Lahiri and Chao Wang, editors, *Computer Aided Verification*, pages 629–652, Cham, 2020. Springer International.
- [6] Oded Goldreich. On Promise Problems (a survey). In *Theoretical Computer Science: Essays in memory of Shimon Even*, pages 254 – 290. Springer, 2006. LNCS. Vol. 3895.

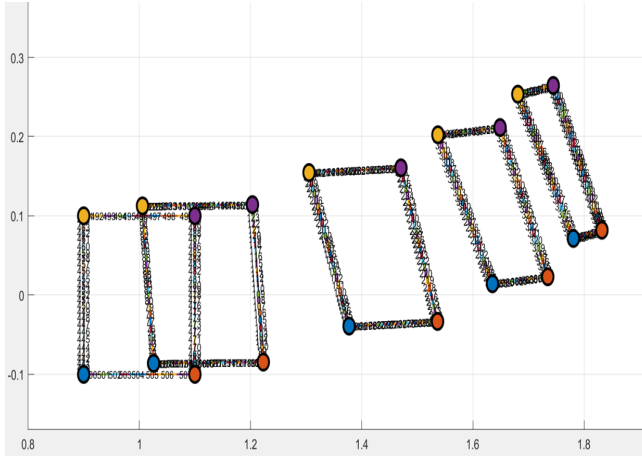


(c) Eg3: Results at  $(T = 0, 0.1, 0.4, 0.7, 1.0)$ . An enlarged view at  $(T = 0.0, 1.0)$  is also shown.

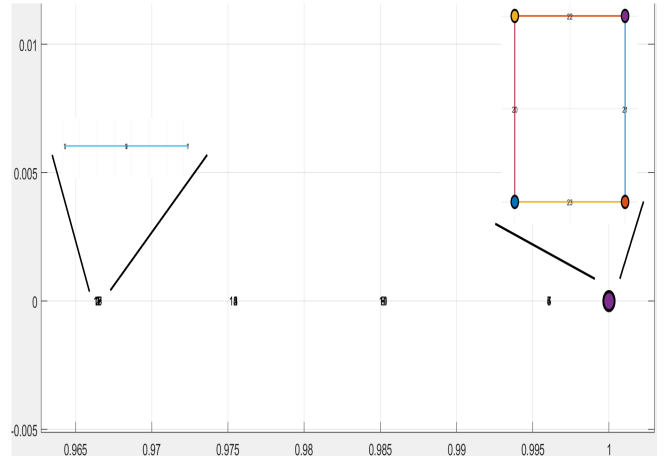


(d) Eg4: Results at  $(T = 0, 0.1, 0.4, 0.7, 1.0)$ . An enlarged view of the connected component at  $(T = 0.0, 0.1)$  is also shown.

**Figure 4: Trajectories and end enclosures for Example Eg3 and Eg4 with  $\varepsilon = 0.01$ .**



(c) Eg5: Results at  $(T = 0, 0.1, 0.4, 0.7, 1.0)$ .



(d) Eg6: Results at  $(T = 0, 0.1, 0.4, 0.7, 1.0)$ . An enlarged view of the connected component at  $(T = 0.0, 1.0)$  is also shown.

**Figure 5: Trajectories and end enclosures for Example Eg5 and Eg6 with  $\varepsilon = 0.01$ .**

- [7] Juan Xu and Chee Yap. Effective subdivision algorithm for isolating zeros of real systems of equations, with complexity analysis. In *Int'l Symp. Symbolic and Alge. Comp.(44th ISSAC)*, pages 355–362, New York, 2019. ACM Press. July 15–18. Beijing.
- [8] N. S. Nedialkov, K. R. Jackson, and G. F. Corliss. Validated solutions of initial value problems for ordinary differential equations. *Applied Mathematics and Computation*, 105(1):21–68, 1999.
- [9] Abraham Galton Bachrach. *Trajectory bundle estimation For perception-driven planning*. Ph.D thesis, M.I.T., 2013.
- [10] K. Tracy, J.Z. Zhang, J. Arrizabalaga, S. Schaal, Y. Tassa3, T. Erez, and Z. Manchester. The trajectory bundle method: Unifying sequential-convex programming and sampling-based trajectory optimization, September 2025.
- [11] T. Kapela, M. Mrozek, D. Wilczak, and P. Zgliczynski. CAPD:DynSys: a flexible C++ toolbox for rigorous numerical analysis of dynamical systems. *Communications in Nonlinear Sci. and Numerical Simulation*, 101:105578, 2021.
- [12] Ernst Hairer, Syvert P. Nørsett, and Gerhard Wanner. *Solving Ordinary Differential Equations I: Nonstiff Problems*. Springer-Verlag, Berlin, second revised edition, 2008.
- [13] John H. Hubbard and Beverly H. West. *Differential Equations, A Dynamical Systems Approach. Part I: Ordinary Differential Equations*. Springer-Verlag, 1991. The 3d Edition (1997) dropped the Part I designation.
- [14] R.E. Moore. Interval Analysis: Differential Equations. In Christodoulous A. Floudas and Panos M. Pardalos, editors, *Encyclopedia of Optimization*, pages 1686–1689. Springer, 2nd edition, 2009.
- [15] Florian Bünger. A Taylor Model Toolbox for solving ODEs implemented in MATLAB/INTLAB. *J. Comp. and Appl. Math.*, 368:112511, 2020.
- [16] William Erik Sherwood. *FitzHugh–Nagumo Model*, pages 1–11. Springer New York, 2013.
- [17] Ernst Hairer and Gerhard Wanner. *Solving Ordinary Differential Equations II: Stiff and Differential-Algebraic Problems*. Springer-Verlag, Berlin, second revised, corrected edition, 2002.

Case	Method	T	$B_1 = (\text{mid}) \pm (\text{rad})$	$\frac{w_{\max}(\text{others})}{w_{\max}(\text{ours})}$	Time (s)
Eg1	Ours	2.00	(0.08, 0.57) $\pm$ (0.02, 0.02)	1	0.02   0.05
	StepB <sub>direct</sub>		(0.08, 0.58) $\pm$ (0.16, 0.13)	6.66	0.52
	VNODE-LP		(0.08, 0.58) $\pm$ (0.04, 0.05)	2.26	0.17
	CAPD		(0.08, 0.58) $\pm$ (0.05, 0.05)	2.12	0.01
	Ours	4.00	(1.46, 0.19) $\pm$ (0.40, 0.05)	1	0.13   0.08
	StepB <sub>direct</sub>		Timeout	N/A	Timeout
	VNODE-LP		(1.43, 0.34) $\pm$ (3.23, 0.91)	8.07	0.39
	CAPD		(1.45, 0.19) $\pm$ (3.38, 0.88)	8.35	0.02
	Ours	5.50	(1.14, 2.95) $\pm$ (0.67, 0.49)	1	3.42   1.21
	StepB <sub>direct</sub>		Timeout	N/A	Timeout
	VNODE-LP		[0.00, 1.09] $\pm$ [4.80 $\times$ 10 <sup>13</sup> , 2.40 $\times$ 10 <sup>13</sup> ]	7.17 $\times$ 10 <sup>13</sup>	5.25
	CAPD		No Output	N/A	No Output
Eg2	Ours	1.00	(-2.13, 0.57) $\pm$ (0.25, 0.21)	1	0.02   0.04
	StepB <sub>direct</sub>		(-2.13, 0.57) $\pm$ (0.26, 0.23)	1.03	0.51
	VNODE-LP		(-2.15, 0.58) $\pm$ (0.90, 3.49)	13.95	0.17
	CAPD		(-2.13, 0.56) $\pm$ (0.29, 0.28)	1.15	0.02
	Ours	2.00	(-1.41, 0.96) $\pm$ (0.38, 0.35)	1	0.77   0.14
	StepB <sub>direct</sub>		Timeout	N/A	Timeout
Eg3	VNODE-LP	1.00	[-2.08, 0.00] $\pm$ [2868.22, 7.88 $\times$ 10 <sup>9</sup> ]	2.07 $\times$ 10 <sup>10</sup>	1.625
	CAPD		No Output	N/A	No Output
	Ours		(-0.60, -6.69) $\pm$ (0.00, 0.18)	1	0.02   0.07
	StepB <sub>direct</sub>		(-0.60, -6.69) $\pm$ (0.01, 0.19)	1.01	4.11
Eg4	VNODE-LP	1.00	(-0.60, -6.69) $\pm$ (0.00, 0.19)	1.05	0.20
	CAPD		(-0.60, -6.69) $\pm$ (0.01, 0.19)	1.01	0.02
	Ours		(0.28, -0.58) $\pm$ (0.15, 0.16)	1	0.01   0.02
	StepB <sub>direct</sub>		(0.28, -0.59) $\pm$ (0.16, 0.17)	1.06	0.01
	VNODE-LP	4.00	(0.28, -0.59) $\pm$ (0.16, 0.18)	1.10	0.03
	CAPD		(0.28, -0.59) $\pm$ (0.16, 0.17)	1.06	0.01
	Ours		(-0.65, 0.25) $\pm$ (0.24, 0.57)	1	0.12   0.06
	StepB <sub>direct</sub>		(-0.68, 0.34) $\pm$ (1.01, 2.12)	3.71	0.01
Eg5	VNODE-LP	1.00	(0.59, 2.53) $\pm$ (22.57, 88.77)	155.74	0.09
	CAPD		(-0.68, 0.34) $\pm$ (7.51, 25.53)	44.79	0.01
	Ours		(1.76, 0.17) $\pm$ (0.11, 0.10)	1	0.03   0.07
	StepB <sub>direct</sub>		(1.76, 0.17) $\pm$ (0.17, 0.10)	1.55	0.01
	VNODE-LP	4.00	(1.76, 0.17) $\pm$ (0.10, 0.10)	0.95	0.09
	CAPD		(1.76, 0.17) $\pm$ (0.18, 0.10)	1.66	0.02
Eg6	Ours	1.00	(1.68, 0.68) $\pm$ (0.08, 0.10)	1	1.22   0.13
	StepB <sub>direct</sub>		Timeout	N/A	Timeout
	VNODE-LP		(1.68, 0.68) $\pm$ (0.07, 0.11)	1.13	0.41
	CAPD	4.00	No Output	N/A	No Output
	Ours		(0.97, 0.00) $\pm$ (0.00, 0.00)	1	15.86   63.35
	StepB <sub>direct</sub>		Timeout	N/A	Timeout
Eg7	VNODE-LP	1.00	(0.97, 0.00) $\pm$ (0.00, 0.00)	1.00	11.06
	CAPD		(0.97, 0.00) $\pm$ (0.00, 0.00)	1.00	16.39
	Ours		(-6.95, 3.00, 35.14) $\pm$ (0.03, 0.01, 0.04)	1	0.12   0.65
	StepB <sub>direct</sub>		(-6.95, 3.00, 35.14) $\pm$ (37.40, 228.27, 225.31)	5692.51	7.35
	VNODE-LP	4.00	(-6.95, 3.00, 35.14) $\pm$ (0.03, 0.01, 0.04)	1.03	0.66
	CAPD		(-6.95, 3.00, 35.14) $\pm$ (0.03, 0.01, 0.04)	1.02	0.10
	Ours		(-4.75, -0.01, 29.07) $\pm$ (0.09, 0.09, 0.11)	1	4.03   12.55
	StepB <sub>direct</sub>		Timeout	N/A	Timeout
Eg8	VNODE-LP	1.00	[ -2.02, -18.46, 6.66 ] $\times$ [ 2.48 $\times$ 10 <sup>7</sup> , 3.09 $\times$ 10 <sup>13</sup> , 3.09 $\times$ 10 <sup>13</sup> ]	2.81 $\times$ 10 <sup>14</sup>	4.90
	CAPD		No Output	N/A	No Output
	Ours		(-1.73, 1.87, 0.03) $\pm$ (0.15, 0.17, 0.00)	1	0.03   0.16
	StepB <sub>direct</sub>		(-1.73, 1.87, 0.03) $\pm$ (0.27, 0.29, 0.00)	1.72	0.01
	VNODE-LP	4.00	(-1.74, 1.86, 0.03) $\pm$ (0.15, 0.18, 0.00)	1.04	0.08
	CAPD		(-1.73, 1.87, 0.03) $\pm$ (0.15, 0.17, 0.00)	1.02	0.02
	Ours		(1.95, -2.89, 0.05) $\pm$ (0.20, 0.23, 0.00)	1	0.08   0.45
	StepB <sub>direct</sub>		(1.95, -2.89, 0.05) $\pm$ (11.67, 8.86, 67.65)	292.99	1.45

**Table 2: Performance comparison of EndCover with existing methods under  $\varepsilon = 1.0$ . For our method, the reported time consists of two values separated by  $a | b$ , where  $a$  denotes the computation time using the End cover and  $b$  denotes the computation time using the Boundary cover. The reported  $B_1$  for our method is obtained by taking the minimal enclosing box of the Boundary cover.**

- [18] O.E. Rössler. An equation for continuous chaos. *Physics Letters A*, 57(5):397–398, 1976.
- [19] Daniel Wilczak and Piotr Zgliczynski.  $C^r$ -Lohner algorithm. *Schedae Informaticae*, 20:9–42, 2011.
- [20] Walter Rudin. *Principles of Mathematical Analysis*. McGraw-Hill, New York, 3rd edition, 1976.

## A Appendix A: Proofs

The numberings of lemmas and theorems in this Appendix are the same as the corresponding results in the text; they are also hyperlinked to the text.

Case	$\varepsilon$	$B_1$	$w_{\max}(B_1)$	Time (s)
Eg1	1.0	$[0.062, 0.092] \times [1.395, 1.532]$	0.137	0.042
	0.5	$[0.062, 0.092] \times [1.395, 1.532]$	0.137	0.042
	0.1	$[0.062, 0.092] \times [1.395, 1.532]$	0.137	0.042
	0.01	$[0.066, 0.089] \times [1.400, 1.527]$	0.126	0.874
Eg2	1.0	$[-2.381, -1.876] \times [0.365, 0.781]$	0.505	0.083
	0.5	$[-2.381, -1.876] \times [0.365, 0.781]$	0.505	0.080
	0.1	$[-2.321, -1.933] \times [0.503, 0.651]$	0.387	0.270
	0.01	$[-2.318, -1.935] \times [0.506, 0.647]$	0.383	3.791
Eg3	1.0	$[-0.601, -0.598] \times [-6.877, -6.508]$	0.369	0.090
	0.5	$[-0.601, -0.598] \times [-6.877, -6.508]$	0.369	0.098
	0.1	$[-0.601, -0.598] \times [-6.872, -6.519]$	0.353	0.293
	0.01	$[-0.601, -0.598] \times [-6.872, -6.519]$	0.352	6.003
Eg4	1.0	$[0.125, 0.434] \times [-0.743, -0.424]$	0.319	0.021
	0.5	$[0.125, 0.434] \times [-0.743, -0.424]$	0.319	0.021
	0.1	$[0.129, 0.432] \times [-0.733, -0.428]$	0.304	0.046
	0.01	$[0.130, 0.432] \times [-0.729, -0.429]$	0.301	0.885
Eg5	1.0	$[1.649, 1.864] \times [0.687, 0.268]$	0.215	0.078
	0.5	$[1.646, 1.866] \times [0.068, 0.268]$	0.220	0.070
	0.1	$[1.678, 1.835] \times [0.070, 0.265]$	0.195	0.169
	0.01	$[1.680, 1.831] \times [0.071, 0.264]$	0.193	2.400
Eg7	1.0	$[-6.976, -6.913] \times [2.986, 3.007] \times [35.104, 35.184]$	0.079	0.647
	0.5	$[-6.976, -6.913] \times [2.986, 3.007] \times [35.104, 35.184]$	0.079	0.647
	0.1	$[-6.976, -6.913] \times [2.986, 3.007] \times [35.104, 35.184]$	0.079	0.647
	0.05	$[-6.976, -6.914] \times [2.987, 3.006] \times [35.105, 35.183]$	0.078	6.083
Eg8	1.0	$[-1.880, -1.588] \times [1.702, 2.039] \times [0.031, 0.035]$	0.337	0.162
	0.5	$[-1.880, -1.588] \times [1.702, 2.039] \times [0.031, 0.035]$	0.337	0.162
	0.1	$[-1.876, -1.591] \times [1.705, 2.036] \times [0.032, 0.035]$	0.331	4.574
	0.05	$[-1.875, -1.592] \times [1.706, 2.036] \times [0.032, 0.035]$	0.329	36.810

Table 3: Performance variation of the algorithm under different tolerance parameters  $\varepsilon$ .

Case	$T$	$Box(\bar{B}_1)$	$\#(\bar{B}_0)$	Time (s)
Eg1	0.5	$[0.152, 0.212] \times [2.170, 2.391]$	8	0.047
	1.0	$[0.062, 0.092] \times [1.395, 1.532]$	8	0.062
	2.0	$[0.064, 0.104] \times [0.553, 0.601]$	8	0.061
	4.0	$[1.052, 1.861] \times [0.136, 0.240]$	12	0.083
Eg2	0.5	$[-2.586, -2.240] \times [0.464, 0.748]$	8	0.044
	1.0	$[-2.3781, -1.876] \times [0.365, 0.781]$	8	0.086
	2.0	$[-1.783, -1.028] \times [0.607, 1.312]$	10	0.152
	4.0	$[1.351, 2.272] \times [-0.343, 2.470]$	56	2.361
Eg3	0.1	$[-1.311, -1.296] \times [3.986, 4.000]$	8	0.050
	0.4	$[-0.941, -0.933] \times [0.398, 0.419]$	8	0.065
	0.7	$[-0.734, -0.729] \times [-1.519, -1.474]$	8	0.073
	1.0	$[-0.601, -0.598] \times [-6.877, -6.508]$	8	0.082
Quadratic	0.5	$[0.503, 0.680] \times [-0.789, -0.581]$	8	0.018
	1.0	$[0.125, 0.434] \times [-0.743, -0.424]$	8	0.024
	2.0	$[-0.620, 0.069] \times [-0.707, -0.314]$	8	0.061
	4.0	$[-0.888, -0.411] \times [-0.318, 0.828]$	11	0.059

Table 4: Performance variation of the algorithm under different time target  $T$ .  $\varepsilon = 1.0$ .

**Theorem 3 (EXISTENCE OF  $f$ -BUNDLES)**

If  $f : \mathbb{R}^n \rightarrow \mathbb{R}^n$  is locally Lipschitz, and  $B \subseteq \text{Valid}_f(H)$ , then the  $f$ -bundle  $\Phi_f(B, H)$  exists.

*Proof.* For each  $\mathbf{p} \in B$ , we have an  $f$ -bundle  $\Phi_f(\text{Ball}_p(r), H)$  for some  $r = r(\mathbf{p}) > 0$  by theorem 1. The union of all these  $f$ -bundles is  $\bar{\Phi}$ , the  $f$ -bundle on  $(\bar{B}, H)$  where  $\bar{B}$  is the union of  $\text{Ball}_p(r(\mathbf{p}))$  for  $\mathbf{p} \in B$ . Since  $B \subseteq \bar{B}$ , the desired bundle  $\Phi_f(B, H)$  is just the restriction  $\bar{\Phi}$  to  $[0, H] \times B$ . **Q.E.D.**

**Theorem 4**

Let  $\Phi : [0, h] \times B \rightarrow \mathbb{R}^n$  be a trajectory bundle where  $B \in \mathbb{R}^n$ . Then the end map  $\text{End}_\Phi$  of (25) is a homeomorphism from  $B$  onto the end-slice  $\Phi|^h$ .

*Proof.* The map (25) has two properties:

- (a) It is continuous (this follows from the continuity of  $\Phi$ ).
- (b) It is injective (this is the stratification property).

If  $U$  is the interior of  $B$ , then Brouwer's Invariance of Domain implies  $U$  is homeomorphic to  $\text{End}_\Phi(U)$ . But the closure of  $\text{End}_\Phi(U)$  is the end-slice  $\Phi|^h$ . Part(b) above says that  $\text{End}_\Phi : B \rightarrow \Phi|^h$  is injective. This implies that  $\text{End}_\Phi$  is a homeomorphism ([20, Theorem 4.17, p.90]). **Q.E.D.**

**Theorem 2**

The set  $\text{Valid}_f(h)$  is an open set for any  $h > 0$ .

*Proof.* Let  $\mathbf{p}^* \in \text{Valid}(h) = \text{Valid}_f(h)$ . It suffices to prove that  $\text{Valid}(h)$  contains an open neighborhood  $U^*$  of  $\mathbf{p}^*$ . Since  $\mathbf{p}^* \in \text{Valid}(h)$ , there is a  $f$ -trajectory  $\phi^*$  with time span  $[0, h]$ . For each  $t \in [0, h]$ , the Picard-Lindelöf Theorem implies that there exists a  $f$ -bundle  $\Phi_t$  on  $[0, \varepsilon(t)] \times B(\phi^*(t), r(t))$ . Since  $f$  is autonomous, we may shift the time-span so that  $\Phi_t$  is a  $f$ -bundle on the cylinder

$$\text{Cyl}(t) = [t, t + \varepsilon(t)] \times \text{Ball}_{\phi^*(t)}(r(t)).$$

Thus the set  $\{(t, t + \varepsilon(t)) : t \in [0, h]\}$  is an open cover of the interval  $[\frac{1}{2}\varepsilon(0), h]$ . By compactness of  $[\frac{1}{2}\varepsilon(0), h]$ , there is a finite set

$$C = \{(t_i, t_i + \varepsilon(t_i)) : i = 0, \dots, m\}$$

that forms a cover of  $[\frac{1}{2}\varepsilon(0), h]$ . Without loss of generality, we may assume that

$$0 = t_0 < t_1 < \dots < t_m < h$$

and the set  $C$  is a minimal cover, i.e., if we omit any  $(t_i, t_i + \varepsilon(t_i))$  from  $C$ , it would not cover  $[\frac{1}{2}\varepsilon(0), h]$ . For each  $i = 1, \dots, m-1$ , choose  $s_i \in (t_{i-1}, t_{i-1} + \varepsilon(t_{i-1})) \cap (t_i, t_i + \varepsilon(t_i))$ . Minimality of  $C$  implies that  $0 < s_1 < s_2 < \dots < s_{m-1} < h$ . Also set  $s_0 = 0$  and  $s_m = h$ .

To prove our theorem, we show how to use the trajectory  $\phi^*$  to construct the open neighborhood  $U^*$ : Recall that  $\Phi_{t_i}$  ( $i = 0, \dots, m-1$ ) is a  $f$ -bundle  $\text{Cyl}(t_i) = [t_i, t_i + \varepsilon(t_i)] \times \text{Ball}_{\phi^*(t_i)}(r(t_i))$ . But since  $[s_i, s_{i+1}] \subseteq [t_i, t_i + \varepsilon(t_i)]$ , we can define  $\Phi_{(i)}$  to be the restriction of

$\Phi_{t_i}$  to the domain  $[s_i, s_{i+1}] \times B_i$  where  $B_i$  is the  $s_i$ -slice of  $\Phi_{t_i}$ . We now have a sequence of  $f$ -bundles

$$\Phi^{(0)}, \Phi^{(1)}, \dots, \Phi^{(m-1)}.$$

Note that the trajectory  $\phi^*$  when restricted to the time-span  $[s_i, s_{i+1}]$  is actually a trajectory of the bundle  $\Phi^{(i)}$ . Let  $B'_i$  denote the end-slice of  $\Phi^{(i)}$ . Then map  $E_i = \text{End}_{\Phi^{(i)}}$  gives us a homeomorphism from  $B_i$  to  $B'_i$ . Moreover,  $B'_i \cap B_{i+1}$  is non-empty since the trajectory  $\phi^*$  passes through them both at time  $s_{i+1}$ :  $\phi^*(s_{i+1}) \in B_{i+1} \cap B'_i$ .

We want to construct a “composition” of the  $E_i$ 's, analogous to  $E_1 \circ E_2 \circ \dots \circ E_m$ . First, let us define  $E_{i-1} * E_i$  (analogous to  $E_{i-1} \circ E_i$ ): from  $E_{i-1} : B_{i-1} \rightarrow B'_{i-1}$  and  $E_i : B_i \rightarrow B'_i$ , we get the homeomorphism

$$E_{i-1} * E_i : E_{i-1}^{-1}(B'_{i-1} \cap B_i) \rightarrow E_i(B'_{i-1} \cap B_i)$$

where we may define  $B_{i-1,i} := E_{i-1}^{-1}(B'_{i-1} \cap B_i)$  and  $B'_{i-1,i} := E_i(B'_{i-1} \cap B_i)$ . Inductively, for  $i = m-1, m-2, \dots, 1$ , define

$$(E_i * \dots * E_m) : B_{i,m} \rightarrow B'_{i,m}$$

where

$$B_{i,m} = E_{i-1}^{-1}(B'_i \cap B_{i+1,m}), \quad B'_{i,m} = E_i(B'_i \cap B_{i+1,m})$$

Thus, the final composition we want is the homeomorphism  $E_1 * \dots * E_m : B_{1,m} \rightarrow B'_{1,m}$  where  $B_{1,m}, B'_{1,m}$  are all open sets **Q.E.D.**

**Lemma 6**

The number of stages in  $\text{EndEncl}(E_0, \varepsilon; \mathbf{p}, H)$  is at most  $1 + \lfloor H/\bar{h} \rfloor$  where  $\bar{h} = \bar{h}(\bar{E}, H, \varepsilon)$ , see (27) and  $\bar{E} = \text{image}(\text{IVP}(E_0, H)) + \text{Box}(\varepsilon)$ .

*Proof.* Since  $\text{IVP}(B_0, H)$  is valid,  $\bar{E}$  is bounded. The set  $\bar{B} = \bar{B}(\bar{E}, H, \varepsilon)$  is also bounded as it is constructed from bounded sets using continuous operations. Since  $f^{[k]}$  is continuous on the compact set  $\bar{B}$ , each  $\bar{M}_i$  ( $i = 1, \dots, n$ ) in the definition (28) of  $\bar{h} = \bar{h}(\bar{E}, H, \varepsilon)$  is finite. Thus,

$$0 < \bar{h} \leq \min_{i=1}^n \left( \varepsilon_i / \bar{M}_i \right)^{1/k}. \quad (30)$$

Suppose the algorithm terminates after  $m$  stages. Then the time sequence of the final scaffold has the form  $\mathbf{t} = (t_0, t_1, \dots, t_m)$  where  $t_0 = 0, t_m = H$ . The  $(j-1)$ th stage was extended to the  $j$ th stage by calling  $\text{StepA}(E_{j-1}, H - t_{j-1}, \varepsilon) \rightarrow (h_j, F_j)$ . Clearly,  $h_j = t_j - t_{j-1}$ . By (27),

$$h_j \geq \min \left\{ H - t_{j-1}, \min_{i=1}^n \left( \frac{\varepsilon_i}{M_i} \right)^{1/k} \right\}.$$

If  $h_j = H - t_{j-1}$ , then  $j$  must be the final stage ( $j = m$ ). Therefore, for every  $j < m$ ,

$$h_j \geq \min_{i=1}^n \left( \frac{\varepsilon_i}{M_i} \right)^{1/k}.$$

We claim that for all  $j = 1, \dots, m-1$ , one has  $h_j \geq \bar{h}$ . This immediately yields

$$(m-1) \bar{h} \leq H, \quad \text{hence} \quad m \leq 1 + \lfloor H/\bar{h} \rfloor.$$

To prove the claim, fix any  $j < m$ . Then

$$\begin{aligned} h_j &\geq \min_{i=1}^n \left( \varepsilon_i / M_i \right)^{1/k} \quad (\text{since } j < m) \\ &\geq \min_{i=1}^n \left( \varepsilon_i / \bar{M}_i \right)^{1/k} \quad (\text{since } M_i \leq \bar{M}_i) \\ &\geq \bar{h} \quad (\text{by definition of } \bar{h}) \end{aligned}$$

The above inequality  $M_i \leq \bar{M}_i$  comes from the inclusion

$$\bar{B}(E_{j-1}, H - t_{j-1}, \varepsilon) \subseteq \bar{B}(\bar{E}, H, \varepsilon),$$

and the definition of  $M_i, \bar{M}_i$  in terms of these two sets. This establishes  $m-1 \leq H/\bar{h}$  as required. **Q.E.D.**

### Lemma 7

Given a scaffold  $\mathcal{S}$  with  $m$  stages and parameters  $\varepsilon > 0$  and  $H > 0$ , the subroutine StepA executed within  $\mathcal{S}.\text{Extend}(\varepsilon, H)$  performs at most

$$\left\lceil \log_2 \left( \frac{H}{\bar{h}} \right) \right\rceil$$

internal iterations, where  $\bar{h} = \bar{h}(E_m(\mathcal{S}), H, \varepsilon)$  is defined in (27).

*Proof.* The Extend subroutine will call StepA. StepA performs a binary search by halving the step size  $H$  until an admissible pair  $(h, F)$  is found. The number of halvings required is  $O(\log_2(H/\bar{h}))$ , as  $H$  is reduced to a minimum viable step size bounded below by  $\bar{h} > 0$ . **Q.E.D.**

### Lemma 8

The modified Refine subroutine terminates.

*Proof.* Suppose, to the contrary, that the modified Refine never terminates. Then it produces infinitely many phases and an infinite sequence of chains

$$C_1 < C_2 < C_3 < \dots,$$

where we write  $C_p = (k(1), k(2), \dots, k(m)) < C_q = (k'(1), k'(2), \dots, k'(m))$  if  $k(i) < k'(i)$  for every  $i = 1, \dots, m$ .

In every phase,  $w_{\max}(E_0(\mathcal{S}))$  is halved whenever Condition 1 (19) fails, and therefore it must eventually satisfy Condition 1 (19). Likewise, for each chain  $C_i$ , the value  $\Delta(C_i)$  is reduced by at least a factor of 2 and hence Condition 2 (20) must eventually be met for all stages as well.

Once both Condition 1 and for all stages Condition 2 hold simultaneously, Condition 3 becomes active, causing Refine to halt. This contradicts the assumption of nontermination. **Q.E.D.**

### Lemma 9

Let  $\mathcal{S}$  be an  $m$ -stage scaffold, and let  $\varepsilon_0 > 0$ . For each stage  $i$  write  $\Delta t_i = t_{i+1}(\mathcal{S}) - t_i(\mathcal{S})$  and

$$G_i(\mathcal{S}) = (\pi_i, \mathbf{g}_i, \bar{\mu}_i^1, \bar{\mu}_i^2, \delta_i, \hat{h}_i, (\ell_i, E_i, F_i)).$$

Let  $I_i = [a, b]$  be an interval satisfies:

$$a = \min_{\mathbf{q} \in \pi(F_i(\mathcal{S}))} (\mu_2(J_{\mathbf{g}_i}(\mathbf{q}))) \quad \text{and} \quad b = \max_{i=1, \dots, m} (\max \bar{\mu}_i^2).$$

Let

$$\bar{\mu} = \max_{i=1, \dots, m} (\max \bar{\mu}_i^1), \quad \Delta_{\max} = \max_{i=1, \dots, m} \delta_i, \quad M_i = \|\mathbf{g}_i^{[2]}(\pi(F_i(\mathcal{S})))\|_2,$$

and define  $\delta'_i = \text{TransformBound} \left( \min \left( \delta_i, \frac{\varepsilon_0}{16m\bar{\mu}} \right), \pi, F_i(\mathcal{S}) \right)$ ,

$$N = \left\lceil \max_{i=1, \dots, m, p \in I_i} \left( \log_2 \left( \frac{\Delta t_i}{h^{\text{euler}}(\Delta t_i, M_i, p, \delta'_i)} \right) \right) \right\rceil. \quad (31)$$

Then the number of phases in  $\mathcal{S}.\text{Refine}(\varepsilon_0)$  is at most

$$1 + \max \left\{ \left\lceil \log_2 \frac{2 w_{\max}(E_0(\mathcal{S})) e^{\bar{\mu}}}{\varepsilon_0} \right\rceil, \left\lceil \log_2 \frac{8m \Delta_{\max} e^{\bar{\mu}}}{\varepsilon_0} \right\rceil + N \right\}.$$

*Proof.* We bound the number of phases required so that condition (19) is satisfied and condition (20) holds for every stage. Then every stage in the next phase will call EulerTube, forming a chain. Then by (15), Refine terminates. The final “+1” in the statement accounts for this last phase.

B1. Phases needed for condition (19). Each phase halves  $w_{\max}(E_0(\mathcal{S}))$ . Thus after

$$\left\lceil \log_2 \frac{2 w_{\max}(E_0(\mathcal{S})) e^{\bar{\mu}}}{\varepsilon_0} \right\rceil$$

phases condition (19) is satisfied.

B2. Phases needed for (20). Fix a stage  $i$ . In each phase, the value  $\delta_i$  is either halved or left unchanged, and once  $\delta_i$  satisfies (20) it will never be modified again. By (20),

$$\delta_i < \frac{\varepsilon_0}{8m\bar{\mu}} \quad \text{and} \quad \delta_i \leq \Delta_{\max},$$

the number of phases in which  $\delta_i$  is halved is at most

$$\left\lceil \log_2 \frac{8m \Delta_{\max} e^{\bar{\mu}}}{\varepsilon_0} \right\rceil.$$

B3. Additional phases from bisection. Recall that during Refine, whenever the logarithmic norm  $\mu$  is positive, we transform the system by  $\pi$ , which yields a new system with a negative logarithmic norm. Hence we have (see [2, Eq. (12)])

$$h^{\text{euler}}(H, \bar{M}, \mu, \delta) = \min \left\{ H, \frac{2\mu\delta}{M(e^{\mu H} - 1) - \mu^2\delta} \right\}.$$

The function  $h^{\text{euler}}(H, \bar{M}, \mu, \delta)$  is decreasing in  $\bar{M}$  and increasing in  $\delta$ . During the refinement, the set  $F_i(\mathcal{S})$  shrinks; therefore

$$M_i = \|\mathbf{g}_i^{[2]}(\pi(F_i(\mathcal{S})))\|_2$$

provides an upper bound for the parameter  $\bar{M}$  in stage  $i$ . Moreover, condition (20) guarantees that  $\min \left( \delta_i, \frac{\varepsilon_0}{16m\bar{\mu}} \right)$  is the lower bound for  $\delta(G_i(\mathcal{S}))$ . So  $\delta'_i$  is an lower bound for the  $\delta$ -parameter in stage  $i$ . Finally, by definition of  $I_i$  the parameter  $\mu$  in  $i$ th stage is always lie in  $I_i$ .

Consequently, for stage  $i$ , the Euler step size has a lower bound  $\min_{p \in I_i} h^{\text{euler}}(\Delta t_i, M_i, p, \delta'_i)$ . Hence the number of required halvings for  $i$ th stage is at most  $\max_{p \in I_i} \left( \log_2 \left( \frac{\Delta t_i}{h^{\text{euler}}(\Delta t_i, M_i, p, \delta'_i)} \right) \right)$

Hence the number of required halvings for every stage is at most  $N$ .

B4. Combining B1, B2 and B3, and adding the final terminating phase, yields the claimed bound. **Q.E.D.**

**Theorem 10**

Let  $\bar{B} = \text{image}(\text{IVP}(B_0, H)) + \text{Box}(\varepsilon)$  and  $\bar{\mu} = \mu_2(J(f(\bar{B})))$ . Then  $\text{EndCover\_Algo}(B_0, H, \varepsilon)$  will call  $\text{EndEncl}$  at most

$$\Theta \left( \left( \frac{2w_{\max}(B_0) e^{\bar{\mu}}}{\varepsilon} \right)^n \right)$$

times.

*Proof.* Each call of  $\text{EndEncl}$  returns two boxes  $\underline{B}_i$  and  $\bar{B}_i$ . We bound the number of indices  $i$  for which the collection  $\{\underline{B}_i\}$  can cover  $B_0$ .

From (19), every box  $\underline{B}_i$  satisfies a uniform positive bound on its size:  $\frac{\varepsilon}{4e^{\bar{\mu}H}} < w_{\max}(\underline{B}_i) < \frac{\varepsilon}{2e^{\bar{\mu}H}}$ . Consequently, starting from a initial box  $B$ , the number of binary subdivisions needed to obtain a box whose size is below this lower bound is at most

$$\left\lceil \log_2 \frac{4w_{\max}(B) e^{\bar{\mu}H}}{\varepsilon} \right\rceil.$$

Hence, along each coordinate direction, the number of such subdivisions is bounded by the above expression. In  $n$  dimensions, it follows that at most

$$O \left( \left( \frac{2w_{\max}(B_0) e^{\bar{\mu}H}}{\varepsilon} \right)^n \right)$$

boxes are created which completes the proof. **Q.E.D.**